Journal of Medicinal Chemistry

Article

Discovery of Potent Cyclophilin Inhibitors based on Structural Simplification of Sanglifehrin A

Victoria A. Steadman, Simon B. Pettit, Karine G. Poullennec, Linos Lazarides, Andrew J. Keats, David K. Dean, Steven J Stanway, Carol A. Austin, Jonathan A. Sanvoisin, Gregory M. Watt, Hans G. Fliri, Albert C. Liclican, Debi Jin, Melanie H. Wong, Stephanie A. Leavitt, Yu-Jen Lee, Yang Tian, Christian R. Frey, Todd C. Appleby, Uli Schmitz, Petr Jansa, Richard L. Mackman, and Brian Edward Schultz

J. Med. Chem., **Just Accepted Manuscript** • DOI: 10.1021/acs.jmedchem.6b01329 • Publication Date (Web): 11 Jan 2017

Just Accepted

ACS Publications

Journal of Medicinal Chemistry is published by the American Chemical Society. 1155 Sixteenth Street N.W., Washington, DC 20036

Discovery of Potent Cyclophilin Inhibitors based on Structural Simplification of Sanglifehrin A

*Victoria A. Steadman,† Simon B. Pettit,† Karine G. Poullennec,†,¶ Linos Lazarides,† Andrew J. Keats,† David K. Dean,† Steven J. Stanway,† Carol A. Austin,† Jonathan A. Sanvoisin,† Gregory M. Watt,†,# Hans G. Fliri,‡ Albert C. Liclican,§ Debi Jin,§ Melanie H. Wong,§ Stephanie A. Leavitt,§ Yu-Jen Lee,§ Yang Tian,§ Christian R. Frey,§ Todd C. Appleby,§ Uli Schmitz,§ Petr Jansa,§ Richard L. Mackman,§ Brian E. Schultz§,**

†Selcia Ltd, Fyfield Business & Research Park, Fyfield Road, Ongar, Essex, CM5 0GS, United Kingdom

‡Cypralis Ltd, Babraham Research Campus, Cambridge, CB22 3AT, United Kingdom

§Gilead Sciences, 333 Lakeside Drive, Foster City, CA 94404, USA

ABSTRACT: Cyclophilin inhibition has been a target for the treatment of hepatitis C and other diseases, but the generation of potent, drug-like molecules through chemical synthesis has been challenging. In this study, a set of macrocyclic cyclophilin inhibitors was synthesized based on the core structure of the natural product sanglifehrin A. Initial compound optimization identified the valine-*m*-tyrosine-piperazic acid tripeptide (Val-*m*-Tyr-Pip) in the sanglifehrin core, stereocenters at C14 and C15, and the hydroxyl group of the *m*-tyrosine (*m*-Tyr) residue as key contributors to compound potency. Replacing the C18-C21 diene unit of sanglifehrin with a styryl group led to potent compounds that displayed a novel binding mode in which the styrene moiety engaged in a π-stacking interaction with Arg55 of cyclophilin A (Cyp A), and the *m*-Tyr residue was displaced into solvent. This observation allowed further simplifications of the scaffold, to generate new lead compounds in the search for orally bioavailable cyclophilin inhibitors.

INTRODUCTION

Cyclophilins are a family of proteins involved in a variety of biological processes. They function as peptidyl-prolyl isomerases[1] but also act as mediators of the immunosuppressive effects of the natural product cyclosporine A (CsA) (Figure 1),[2, 3] and as chaperone proteins. CsA, a macrocyclic oligopeptide, exerts its immunosuppressive effects through binding to the active site of cyclophilins and simultaneously interacting with the protein calcineurin. (Me-Ile-4) cyclosporine (NIM811), a cyclosporine isolated from *Tolypocladium niveum*, displayed strong inhibition of cyclophilin but lacked the ability to bind calcineurin, and therefore, lacked immunosuppressive properties.[4, 5] This discovery prompted further studies aimed at interrogating

the biological role of cyclophilin inhibition without immunomodulation and connected the function of some family members to disease states such as asthma, inflammation, ischemia/reperfusion, fibrosis, viral diseases, and cancer.[6-8] More recently, the sanglifehrins, natural products isolated from *Actinomyces* bacteria, have also been reported to bind to cyclophilins and demonstrate similar immunosuppressive properties to those of CsA.[9-11] In contrast to the macrocyclic oligopeptide of CsA, the sanglifehrins are macrocycles containing a valine-*meta*-tyrosine-piperazic acid (Val-*m*-Tyr-Pip) tripeptide motif as well as an extended polyketide structure (Figure 1).

Beyond the early interest in using non-immunosuppressive cyclophilin inhibitors to target human immunodeficiency virus (HIV),[12] cyclosporine derivatives have played a prominent role in the race for pan-genotypic hepatitis C virus (HCV) antivirals. Involvement of cyclophilins in the life cycle of hepatitis C was first identified based on the efficacy of CsA against hepatitis C virus in infected hepatocytes, and in HCV replicon assays.[13] Knockdown experiments utilizing RNA interference identified Cyp A as the key cyclophilin necessary for HCV replication, with no significant contribution from cyclophilins B and C.[14, 15] A combination of viral resistance selections and biophysical studies has identified the non-structural protein NS5A of HCV as the principal viral protein to which Cyp A binds,[16-19] but the exact mechanism by which this interaction facilitates viral replication remains unclear. Cyp A is a desirable target for HCV treatment on account of the efficacy of cyclophilin inhibitors against all genotypes of hepatitis C,[20-22] and the probable high barrier to the development of viral resistance. Importantly, clinical proof of concept studies with the non-immunosuppressive CsA analog alisporivir (Figure 1) demonstrated significant anti-HCV activity before its development was put on hold due to toxicity observed when dosed in combination with ribavirin and pegylated interferon.[23] On the

heels of this molecule, the CsA analog SCY-635[24-26] (Figure 1) also progressed to early clinical studies for the treatment of HCV. Not surprisingly, the sanglifehrins have also been explored as potential anti-HCV agents. Degradation studies on sanglifehrin A determined that removal of the C24 polyketide side chain eliminated the immunosuppressive properties of the molecule[27] while retaining the nanomolar binding affinity to cyclophilin A, B, and C.[15] Moreover, a degradation product from these studies was subjected to further chemical synthesis to yield AAE931 (**1**, Figure 1), a compound that showed potent anti-HCV activity in the replicon assay (EC_{50} = 130 nM).[15, 28] Subsequently, researchers at Biotica have bioengineered the polyketide pathways to provide a variety of sanglifehrin analogs such as NVP018 (Figure 1) as potential oral cyclophilin inhibitors for the treatment of HCV and other diseases.[29-32]

Our long-term endeavor was to develop a small molecule cyclophilin inhibitor derived solely through chemical synthesis that would possess excellent oral pharmacokinetics with no drug-drug interactions. Such an inhibitor would then be amenable to co-formulation with other direct acting oral HCV antivirals such as sofosbuvir[33] to generate a pan genotypic fixed dose oral regimen for the treatment of HCV. To date, drug discovery programs based on classical small-molecule library screening and lead optimization have not been reported to result in late-stage cyclophilin inhibitors with optimized oral pharmacokinetic properties. We conducted a pilot screen on ~19,000 library compounds and did not discover compounds that were promising Cyp A inhibitors in a time-resolved fluorescence resonance energy transfer (TR-FRET)-based binding assay. Therefore, our attention turned to a strategy of simplification of the sanglifehrin-derived molecule **1** that demonstrated potent cyclophilin inhibition and anti-HCV activity. The total synthesis of sanglifehrin A was reported by two groups[34-36] and provided the groundwork for this effort. However, a projected total synthesis of **1** would still require almost 40 synthetic steps!

Sedrani et al. synthesized a series of sanglifehrin analogs with reduced complexity via ring-closing metathesis. [27, 37, 38] Multiple chemical changes were made in each of the reported analogs compared to **1** and the result was an approximate 1000-fold drop in potency. Despite this result, we reasoned based on structural analysis of both the sanglifehrin A complex and compound **2**, a close analog of **1**, that the generation of potent simplified sanglifehrins should be feasible (Figure 2). A key part of the strategy which differed from the previous report was retaining the Val-*m*-Tyr-Pip tripeptide that forms several hydrogen bonding interactions within the active site. Iterative simplifications of **1**, guided by a combination of biological, biophysical, and crystallographic data, led to the generation of compounds **3-9**. Compounds **8** and **9** are surprisingly simple, low molecular weight, synthetically tractable molecules that have demonstrated potent inhibition of cyclophilin A and antiviral activity in the HCV replicon assays.

RESULTS AND DISCUSSION

The crystal structure of compound **2** bound to cyclophilin A[27] showed a binding geometry nearly identical to that of the macrocyclic core of sanglifehrin A (Figure 3). Both of the piperazic acid and *m*-Tyr amino acids make hydrogen bonds with the cyclophilin protein, suggesting that both are likely critical for achieving potency. In contrast, the C23 and C14 side chains do not form hydrogen bonds suggesting they may be dispensable. Therefore, the first simplified target to validate this structural hypothesis was compound **3**, containing the diene at C18-C21 and the four chiral centers found at C14-C17 in sanglifehrin (Scheme 1). Because the two hydroxyls at C15 and C17 of **2** appeared to not make direct interactions with the protein, we chose to cap them with methyl groups to simplify the protecting group strategy. Our synthetic approach to compound **3** centered on RCM at C20-C21 unlike the simplified analogs reported earlier[27]

(Scheme 1). The synthesis of **3** began with known diol **10**, which was prepared using Paterson's methodology in 5 steps in high yield.[39] Methylation of **10** followed by debenzylation and reprotection of the resulting alcohol provided the pivaloyl ester **11**. Ozonolysis of the alkene and condensation of the resulting aldehyde with diethyl allyl phosphonate afforded the terminal diene **12**. Hydrolysis of the ester followed by a 2 step oxidation furnished the carboxylic acid **13**. Peptide **15** was prepared from the Val-*m*-Tyr-Pip tripeptide **14**[27] by hydrolysis of the TCE ester and re-esterification with homoallyl alcohol via an acid anhydride. Deprotection of the Boc group followed by an HATU mediated coupling with acid **13** then afforded the RCM precursor **16**. Ring closing metathesis using Grubbs I followed by TBAF mediated silyl group removal provided **3**.

The removal of the C16 and C17 stereocenters for target compounds **4** and **6-7** shortened the synthesis of this region of the macrocycle to only a few steps (Scheme 2). Silyl enol ether formation on Oppolzers sultam **17** was followed by $TiCl_4$ mediated anti-aldol reaction with 4-pentenal to provide alcohol **18** with complete stereocontrol. Methylation of the alcohol and hydrolysis of the chiral auxiliary afforded the desired acid **19**. In contrast to the route described for compound **3**, we preferred the C18-C19 ring closure for these targets since this enabled the evaluation of different diene replacements e.g. aryl alkenes **6-7.** With **19** in hand**,** the RCM precursors **25-27** were readily generated from the tripeptide TCE ester **14.** First, removal of the TCE group was followed by coupling with (*E*)-hexa-3,5-dien-1-ol to provide **22**, while EDC mediated coupling with benzyl alcohol **21** provided **24**. Intermediate **23** was prepared directly from the TCE ester **14** by base mediated transesterification with 3-vinyl benzyl alcohol. Boc removal on intermediates **22-24** and either HATU or EDC mediated coupling with carboxylic acid **19,** generated the desired precursors **25-27** for the RCM**.** Grubbs I catalyst mediated closure

of the ring followed by silyl deprotection resulted in targets **4**, **6**, and **7** respectively, in moderate to good yield without significant optimization.

Compound **5** lacking all C14-C17 functionality was first described by Novartis and was prepared following the literature procedure (compound 47d[27]).

Lastly, compounds **8** and **9** with an alanine in place of *m*-Tyr (Scheme 3) required a different sequence of steps but ultimately converged to the same C18-C19 RCM reaction. Coupling of piperazic TCE ester **28**[37] with Boc protected alanine, followed by Boc deprotection and subsequent coupling with Boc-valine afforded the protected tripeptide **29** in good yield. Deprotection of the terminal Boc group and HATU coupling with acid **19** or hept-6-enoic acid gave intermediates **30** and **31** respectively. Base hydrolysis of the TCE ester and subsequent EDC coupling with chiral alcohol **21** furnished the RCM precursors **32** and **33**. In this example, Hoveyda-Grubbs II catalyst proved higher yielding than Grubbs I to give the targets **8** and **9** in 28% and 22% yield respectively.

The binding affinity of compounds **3-9** for cyclophilin A was measured using a competitive binding TR-FRET assay, and was corroborated with a functional peptidyl-prolyl isomerase (PPIase) assay. Antiviral activity was measured using a hepatitis C genotype 1b replicon assay in Huh7 cells (Table 1). For all compounds, antiviral activity generally paralleled compound binding affinity to Cyp A.

Compound **3** showed strong binding to Cyp A (K_d = 25 nM) and submicromolar anti-viral activity in the HCV replicon cellular assay (EC_{50} = 600 nM). Capping the C15 and C17 hydroxyls was therefore tolerated, and the truncation of the side chains at C14 and C23 had a minimal effect on biochemical potency (the reported K_d values for Cyp A binding for sanglifehrin A, **1**, and **2** are single-digit nanomolar[27]). The activity of the additional diene

compounds **4** and **5** demonstrated the effect of sequential removal of the stereocenters in the C14-C17 region. Compound **4**, with only the C16 and C17 substituents removed, showed potency nearly equal to that of compound **3** in the cyclophilin binding assay (K_d = 65 nM), with slightly better anti-viral activity (EC_{50} = 240 nM). This result suggested that the chiral centers at C16 and C17 in compound **3** are not essential for activity, an observation that enabled us to reduce the complexity of subsequent target molecules. Compound **5**, which lacks all four C14-C17 stereocenters present in compound **3**, showed a dramatic decrease in potency, yielding a K_d value of 2.6 μM against Cyp A. Compound **5** was previously reported by Novartis to have single-digit micromolar activity[37] consistent with our findings. The low biochemical potency also translated to a low cellular potency (EC_{50} = 4.5 μM). The retained potency of compound **4** bearing only 2 stereocenters at C14 and C15 was surprising when considering the set of very similar macrocycles reported earlier that showed micromolar binding affinities when the three C14-C16 stereocenters were retained.[27] However, compared to those synthetic macrocycles, compound **4** contained the *m*-Tyr residue, suggesting that the *m*-Tyr residue and the C14-C15 stereocenters are sufficient to obtain good binding potency and submicromolar replicon activity in the diene containing compounds.

To elucidate the structural basis for the effects rendered by the C14-C17 sidechains, we determined X-ray crystal structures for compounds **3** and **5** bound to cyclophilin A. Not surprisingly, the more potent compound **3** exhibits a binding mode almost identical to that observed for sanglifehrin A and **2**. The RMSD for all shared heavy atoms vs sanglifehrin A is 0.44 Å and 0.56 Å vs **2**, respectively (Figure 4). This suggests that more elaborate C14 and C23 sidechains as well as the methylated C15 and C17 hydroxyls have little influence on the macrocycle's conformation itself. As described previously,[27] the Val-*m*-Tyr-Pip tripeptide

moiety is the most buried portion of the inhibitor and is responsible for making all of the hydrogen bonding interactions observed between the ligand and enzyme based on heavy atom distances (2.7-3.0 Å). The four carbon atoms of the piperazic acid bind in a deep hydrophobic pocket formed by Phe 60, Met 61, Leu 122, and Phe113. The backbone carbonyl oxygen of the Val residue forms a hydrogen bond with the side chain nitrogen (NE2) of Gln 63. A pair of hydrogen bonds is observed between backbone atoms of the tripeptide *m*-Tyr and Asn 102 of the enzyme. The side chain carbonyl oxygen (OE2) of the Gln63 also participates in hydrogen bonding with the α-nitrogen of the piperazic acid. The most solvent-exposed hydrogen bond is formed by the hydroxyl oxygen of the *m*-Tyr and the His 126 (NE) side chain atoms. In addition to these direct protein-ligand interactions, there is an additional solvent-mediated hydrogen bond between the Val carbonyl oxygen of the tripeptide and a structurally conserved water molecule which is in turn coordinated by three different protein residues (His 54, Arg 55, and Gly 72). For the 40-fold less potent compound **5** that lacks the C14-C17 stereocenters, the binding mode of the Val-*m*-Tyr-Pip tripeptide portion is very well conserved, indicated by a heavy atom RMSD of 0.27 Å to sanglifehrin A. However, the conformation of the non-peptidic C14-C23 moiety is different, with an RMSD of 1.05 Å to sanglifehrin A, compared to an RMSD of only 0.44Å for compound **2**. (This difference results in a loss of ~40Å^2 of total buried surface area compared to compound **2**).

With respect to the cyclophilin structure itself for the crystal structures of compounds **3** and **5**, there are no remarkable differences when compared to the complex of **2** (heavy atom RMSD for protein residues within 5 Å of ligands is 0.33 and 0.36 Å, respectively) (Figure 4).

One molecular feature that sets compound **3,** along with sanglifehrin A and **2**, apart from compound **5** is the observation of the intramolecular hydrogen bond between the amide nitrogen

of the valine residue and the oxygen at C15 (Figure 5). Analysis of *in silico* conformational models for compounds **3** and **5** showed that the intramolecular hydrogen bond is maintained in 43% of low energy conformers (<10 kcal) while the corresponding backbone conformation for compound **5** is seen in less than 5% of conformers (Supporting Information Figure S1).

With this potential conformational bias for compound **3**, we probed the thermodynamic basis for the trend in potency using isothermal calorimetry (ITC) and variable-temperature surface plasmon resonance (SPR). Results are shown in Table 2. The binding of compound **3** was driven predominantly by enthalpy, with a contribution of -10.0 kcal/mol from enthalpy and -0.3 kcal/mol from entropy, based on the ITC data. The SPR data showed a similar pattern. For compound **4**, a ΔH value of -8.6 kcal/mol was measured by ITC, with the $-(T\Delta S)$ contribution of -0.9 kcal/mol. For compound **5**, the decrease in biochemical potency was driven by ΔH, with a value of -7.0 kcal/mol from the ITC experiments. The $-(T\Delta S)$ component of binding was -1.2 kcal/mol. The thermodynamic values from the SPR experiments for compounds **3-5** were consistent with those from the ITC measurements. That the differences in ΔG for binding of compounds **3-5** to Cyp A primarily reflected changes in enthalpy might seem surprising given that conformational bias is typically related to an entropic contribution. However, an increased enthalpic contribution for compound **3** is most likely due to transferring non-hydrogen bonded solution conformers into the hydrogen-bonded, bound conformation.

We then explored further rigidification of the non-peptidic portion by modifying the diene moiety. Modeling studies suggested that a meta-substituted styryl group could be introduced into the C18-C22 region, leading to compound **6** as a target. Indeed compound **6** was found to maintain high potency in the biochemical and cellular assays (K_d = 64 nM; EC_{50} =320 nM).

The co-crystal structure of compound **6** with cyclophilin A shows some significant changes in binding mode driven by the presence of the styrene unit (Figure 6). Besides a significant *m*-Tyr side chain rotation of approximately 100º (about χ_1) that eliminated the hydrogen bond with His 126, the styrene moiety makes a different interaction with Arg 55. The overlay with the compound **3** co-crystal structure in Figure 5 shows that the edge-on hydrophobic interaction of the diene moiety has been replaced with a tight π–stacking interaction of the styrene with the π–face of the guanidinium-group of Arg 55. In light of the very similar potencies of compounds **3**, **4**, and **6**, it seems that the contribution of the *m*-Tyr side chain interaction with His 126 can be compensated by this new interaction between the styrene group and Arg 55. The position of the *m*-Tyr side chain seems to represent a hydrophobic collapse of the ligand itself, defined by intramolecular hydrophobic packing of *m*-Tyr phenyl moiety against the edge of the styrene group and the apolar side of the C13-carbonyl. This binding mode represents maximal hydrophobic surface burial for the ligand, leaving the *m*-Tyr hydroxyl available to interact with bulk solvent.

For further compound optimization, we chose to introduce a C23-methyl substituent as a simplified version of the side chains present in sanglifehrin and **1**, synthesizing compound **7**. Compound **7** showed improved biochemical potency (K_d = 11 nM) as well as greater cellular potency (EC_{50} = 36 nM) than compound **6**. The crystal structures for compounds **6** and **7** did not offer a clear explanation for this potency improvement, showing practically identical binding modes (Figure 7A), including the side chain conformation for the *m*-Tyr. It appears that the C23 methyl group engages in a hydrophobic interaction with the side chains of Ile 57 and Phe 60, which may contribute to the increase in potency. The C23 methyl group was incorporated into all subsequent analogs due to its improved potency. It is noteworthy that all of the reported potent

sanglifehrins and sanglifehrin derivatives[10, 11, 15, 27, 29-31, 40] possess the unusual amino acid *m*-Tyr, suggesting that this moiety is necessary for potent binding. However, the X-ray structure of compounds **6** and **7** strongly suggested that the *m*-Tyr side chain may be dispensable for binding when the styryl group is present, prompting the synthesis of compound **8** containing an alanine residue instead of *m*-Tyr. Compound **8** had a remarkable biochemical K_d value of 24 nM and a cellular EC_{50} value of 87 nM, confirming that the *m*-Tyr sidechain was dispensable in the context of the novel styrene binding mode. The importance of this switch, beyond providing a simpler, more efficient synthesis using a natural amino acid, is the removal of possible metabolic liabilities of the *m*-Tyr group such as glucuronidation and aromatic oxidation.

The co-crystal structure of compound **8** bound to cyclophilin A is shown in Figure 7B. The ligand binding mode of compound **8** is remarkably similar to that of compounds **6** and **7**. However, the absence of the *m*-Tyr sidechain leads to a significant change in the C16-C19 linker (aromatic) region. The styrene group is now flipped down toward the bottom of the pocket, making a tighter hydrophobic interaction with the π-face of the Arg55 guanidinium group. Notably, the C23-methyl group has moved slightly away from the Ile57/Phe60 hydrophobic shelf. The co-crystal structure of compound **7** shows that the hydrophobic interactions of the non-peptidic linker moiety are essential for binding to the cyclophilin A pocket with Arg55 emerging as a key residue.

To verify that this simplified scaffold lacked immunosuppressive properties, compounds **4** and **8** were chosen for testing in a four-day FACS-based T cell proliferation assay. In this assay, the control compound CsA inhibited proliferation with an EC_{50} value of 6.4 ± 2.5 nM, consistent with reported literature values using a radiometric T cell proliferation assay.[11] However,

compounds **4** and **8** yielded EC_{50} values >10 μM, suggesting that these compounds are not immunosuppressive.

The final key question remaining was whether the stereocenters at C14 and C15 were also essential for potency in the styrene series. Compound **9** was prepared and showed only a 2-fold drop in the binding affinity compared to **8** and equivalent functional activity. Thus by iterative structure based SAR the synthetic complexity and challenges associated with compound **3** containing the diene, C14-C17 stereocenters, and the *m*-Tyr were all removed in arriving at compound **9**. These realizations and the new crystallographic binding mode opened up many more design possibilities to optimize the absorption and metabolic properties of these simplified sanglifehrins to afford good oral bioavailability. In addition, the π-stacking interactions between the styrene residues and Arg55 reveal an additional avenue for compound optimization.

CONCLUSION

The potential utility of non-immunosuppressive cyclophilin inhibitors for the treatment of a variety of diseases has been recognized for over twenty years, but to date it has been very challenging to generate potent, drug-like cyclophilin inhibitors through chemical synthesis. Utilizing the sanglifehrin natural product, we have applied focused medicinal chemistry informed by critical insights gained from crystallography and biophysical studies to address this problem. The synthesis and systematic analysis of compounds modifying the macrocyclic core of sanglifehrin has resulted in the first potent and synthetically tractable inhibitors of cyclophilins. For macrocycles retaining the the diene unit of sanglifehrin, we were able to reduce the complexity of the molecules and determine that the presence of the *m*-Tyr along with the C14 and C15 stereocenters was sufficient to maintain potency. The dramatically different binding mode observed for macrocycles containing the styrene unit was a further breakthrough in

generating simple, potent cyclophilin inhibitors. This new binding mode, based on the π-stacking of the aromatic unit at C20-22 with R55 of cyclophilin A, enabled a second generation of analogs in which the *m*-Tyr was replaced with alanine and all of the C14 to C17 stereocenters were removed without loss of potency. These findings have provided new, more synthetically tractable leads for the design of potent, orally bioavailable small-molecule cyclophilin inhibitors that lack immunosuppressive properties. Indeed, more than 400 synthetic macrocyclic cyclophilin inhibitors that were potent in biochemical and anti-viral assays were generated as a result of this discovery.[41-44] With these compounds, the biology of cyclophilin inhibition as it relates to disease states may now be interrogated more effectively.

EXPERIMENTAL SECTION

Proton Magnetic Resonance (NMR) spectra were recorded on a Bruker instrument at 300, 400 or 500 MHz. Chemical shifts are reported in ppm (δ) using the residual solvent line as internal standard. Splitting patterns are designed as s, singlet; d, doublet; t, triplet; q, quartet; m, multiplet; b, broad.

LC/MS Data were generated on a Waters ZQ Mass Spectrometer, operating in switched ES+ and ES- ionization modes coupled to an Agilent 1100 Series HPLC system with in line Aglient 1100 UV-DAD and Sedere SEDEX 75 ELSD Detection. Instrument control and data acquisition is mediated through the Waters MassLynx – OpenLynx software suite. Retention times are denoted as Tr.

All isolated characterized compounds were determined to have a purity of >95% by LC-MS and NMR.

Compounds **5**,[27], **10**,[39] **14**,[27] and **28**[37] were prepared as described in the literature. Compounds **17** and **20** were purchased from commercial sources.

(13*E*,15*E*)-(3*S*,6*S*,9*R*,10*R*,11*S*,12*S*,21*S*)-3-(3-Hydroxy-benzyl)-6-isopropyl-10,12-dimethoxy-9,11-dimethyl-19-oxa-1,4,7,25-tetraaza-bicyclo[19.3.1]pentacosa-13,15-diene-2,5,8,20-tetraone (3)

A solution of **16** (228.7 mg, 0.291 mmol) in dry dichloromethane (150 mL) was treated with Grubbs' first generation catalyst (47.9 mg, 0.058 mmol). After stirring at reflux for 18 h, more Grubbs' first generation catalyst was added (47.9 mg, 0.058 mmol). After stirring for 2 h at reflux, the reaction was cooled to room temperature and polymer-supported methylthiourea was

added (1.5 g). After stirring for 24 h at room temperature, the mixture was filtered through Celite and the volatiles were removed *in vacuo*. The residue was subjected to silica gel chromatography using a 25 g Isolute cartridge eluted with a continuous gradient of *iso*-hexane/ethyl acetate 1:0 to 1:4 to afford the crude macrocycle (71.8 mg) which was dissolved in anhydrous tetrahydrofuran (8 mL) and treated with a solution of tetrabutylammonium fluoride (1 M in tetrahydrofuran, 0.5 mL, 0.5 mmol). After stirring at room temperature for 40 min more tetrabutylammonium fluoride was added (1 M in tetrahydrofuran, 0.5 mL, 0.5 mmol). After stirring at room temperature for 18 h, the volatiles were removed *in vacuo* and the residue was purified by silica gel chromatography using a 10 g Isolute cartridge eluted with a continuous gradient of *iso*-hexane/ethyl acetate 1:0 to 0:1 to afford the title compound (26.3 mg, 14% over 2 steps) as a yellow solid. ^{1}H NMR (300 MHz, d_6-DMSO) δ 9.14 (s, 1H), 8.04 (d, J = 7.3 Hz, 1H), 7.06–6.95 (m, 2H), 6.66–6.48 (m, 4H), 6.19–6.04 (m, 2H), 5.56–5.27 (m, 3H), 4.84 (d, J = 11.3 Hz, 1H), 4.29–4.19 (m, 1H), 4.18–3.99 (m, 3H), 3.18 (s, 3H), 3.04 (s, 3H), 2.81–2.61 (m, 3H), 2.45–2.37 (m, 1H), 2.35–2.25 (m, 1H), 1.94–1.74 (m, 2H), 1.73–1.55 (m, 3H), 1.53–1.39 (m, 1H), 1.38–1.26 (m, 1H), 1.13 (d, J = 7.7 Hz, 3H), 0.86 (d, J = 6.8 Hz, 3H), 0.80 (d, J = 6.8 Hz, 3H), 0.67 (d, J = 6.8 Hz, 3H). LC/MS (*m/z*) 665.4 [M+Na], Tr = 4.78 min.

(13*E*,15*E*)-(3*S*,6*S*,9*R*,10*R*,21*S*)-3-(3-Hydroxy-benzyl)-6-isopropyl-10-methoxy-9-methyl-19-oxa-1,4,7,25-tetraaza-bicyclo[19.3.1] pentacosa-13,15-diene-2,5,8,20-tetraone (4)

A solution of **25** (133 mg, 0.180 mmol) in dichloromethane (85 mL) was prepared and Grubbs 1st generation catalyst (45 mg, 0.054 mmol) was added. The stirred reaction mixture was heated at reflux for 36 h then cooled to room temperature. Silica gel was added and the mixture was evaporated to dryness. The residue was purified by silica gel chromatography eluting with a

stepwise gradient of *iso*-hexane/ethyl acetate 1:0 to 0:1 to yield (13*E*,15*E*)-(3*S*,6*S*,9*R*,10*R*,21*S*)-3-[3-(*tert*-butyl-dimethyl-silanyloxy)-benzyl]-6-isopropyl-10-methoxy-9-methyl-19-oxa-1,4,7,25-tetraaza bicyclo[19.3.1]pentacosa-13,15-diene-2,5,8,20-tetraone (38 mg, 30%) as a dark brown solid. ^{1}H NMR (300 MHz, $CDCl_3$) 7.20–7.05 (m, 1H), 6.97 (d, J = 9.1 Hz, 1H), 6.80 (d, J = 7.6 Hz, 1H), 6.74–6.52 (m, 3H), 6.47 (d, J = 8.0 Hz, 1H), 6.20–5.98 (m, 2H), 5.80–5.49 (m, 3H), 4.55–4.44 (m, 1H), 4.41–4.20 (m, 2H), 4.19–4.02 (m, 2H), 3.52 (d, J = 12.0 Hz, 2H), 3.47 (s, 1H), 3.41–3.09 (m, 2H), 2.96–2.72 (m, 2H), 2.70–2.29 (m, 4H), 2.28–1.94 (m, 4H), 1.88–1.39 (m, 6H), 1.38–1.20 (m, 4H), 0.99 (s, 9H), 0.94 (d, J = 6.7 Hz, 3H), 0.19 (s, 6H). LC/MS (*m/z*) 713.4 [M+H], Tr = 5.6 min.

A stirred solution of (13*E*,15*E*)-(3*S*,6*S*,9*R*,10*R*,21*S*)-3-[3-(*tert*-butyl-dimethyl-silanyloxy)-benzyl]-6-isopropyl-10-methoxy-9-methyl-19-oxa-1,4,7,25-tetraaza bicyclo[19.3.1]pentacosa-13,15-diene-2,5,8,20-tetraone (38 mg, 0.053 mmol.) in anhydrous tetrahydrofuran (10 mL) was cooled to 0 °C under a nitrogen atmosphere before adding tetrabutylammonium fluoride (1 M in tetrahydrofuran, 265 µL, 0.265 mmol). The reaction mixture was warmed to room temperature and was stirred under a nitrogen atmosphere for 2.5 h. The reaction mixture was then treated with saturated sodium bicarbonate solution (20 mL) and the aqueous layer was extracted with ethyl acetate (3 × 15 mL). The combined extracts were dried over anhydrous sodium sulfate, filtered, and evaporated. The residue was purified by silica gel chromatography eluting with a stepwise gradient of *iso*-hexane/ethyl acetate 1:1 to 0:1 to yield the title product (15 mg, 47%) as a colorless solid. ^{1}H NMR (300 MHz, $CDCl_3$) 8.38–8.15 (m, 1H), 7.41 (d, J = 9.6 Hz, 1H), 7.08 (t, J = 7.7 Hz, 1H), 6.85 (d, J = 8.7 Hz, 1H), 6.78–6.68 (m, 2H), 6.58–6.51 (d, J = 7.4 Hz, 1H), 6.00–5.91 (m, 3H), 5.69–5.43 (m, 3H), 4.55 (d, J = 12.7 Hz, 1H), 4.40–4.09 (m, 4H), 3.56 (d, J = 12.5 Hz, 1H), 3.52 (s, 3H), 3.30–3.18 (m, 2H), 2.92–2.75 (m, 2H), 2.71–2.55 (m, 2H), 2.53–

2.38 (m, 2H), 2.19 (s, 1H), 2.10–1.45 (m, 6H), 1.36 (d, *J* = 7.4 Hz, 3H), 1.01–0.93 (m, 4H), 0.92–0.81 (m, 3H). LC/MS (*m/z*) 599.4 [M+H], Tr = 4.59 min.

(*E*)-(5*S*,11*S*,14*S*,17*R*,18*R*)-11-(3-Hydroxy-benzyl)-14-isopropyl-18-methoxy-17-methyl-3-oxa-9,12,15,28-tetraaza-tricyclo[21.3.1.1^{5,9}]octacosa-1(27),21,23,25-tetraene-4,10,13,16-tetraone (6)

To **26** (280 mg, 0.36 mmol) in anhydrous dichloromethane (120 mL) was added Grubbs 1st generation catalyst (89 mg, 0.11 mmol). The reaction was heated to reflux for 16 h. The reaction was cooled and concentrated *in vacuo*. The product was purified by silica gel chromatography eluting with a stepwise gradient of *iso*-hexane/ethyl acetate 1:1 to 1:2 to afford (*E*)-(5*S*,11*S*,14*S*,17*R*,18*R*)-11-[3-(*tert*-Butyl-dimethyl-silanyloxy)-benzyl]-14-isopropyl-18-methoxy-17-methyl-3-oxa-9,12,15,28-tetraaza-tricyclo[21.3.1.1^{5,9}]octacosa-1(27),21,23,25-tetraene-4,10,13,16-tetraone (213 mg, 75%) as a brown oil that solidifies under vacuum. To the resulting residue (70 mg, 0.09 mmol), was added anhydrous tetrahydrofuran (1 mL) and cooled to 0 °C. A solution of tetrabutylammonium fluoride (0.5 mL, 0.47 mmol, 1.0 M in tetrahydrofuran) was added and the reaction was stirred at 0 °C for 0.5 h. The reaction was quenched with aqueous saturated ammonium chloride and extracted with dichloromethane (2×). The combined organic layers were filtered through a hydrophobic frit and concentrated *in vacuo*. The product was purified by silica gel chromatography eluting with a stepwise gradient of *iso*-hexane/ethyl acetate 1:1 to 1:2 to afford the title product (25 mg, 44%) as a white solid. ^{1}H NMR (300 MHz, d_6-DMSO) δ 8.10 (*br* s, 1H), 7.41–7.21 (m, 3H), 7.21–7.16 (m, 1H), 7.12–7.05 (m, 1H), 6.94–6.89 (m, 1H), 6.85–6.76 (m, 1H), 6.72–6.63 (m, 2H), 6.50–6.43 (m, 1H), 6.10–6.04 (m, 2H), 5.78–5.68 (m, 1H), 5.21 (s, 2H), 4.62–4.52 (m, 1H), 4.27–4.18 (m, 1H), 3.67 (d, *J* = 12.2 Hz, 1H),

3.50 (s, 3H), 3.43–3.24 (m, 2H), 2.74–2.58 (m, 2H), 2.26–1.91 (m, 5H), 1.82–1.55 (m, 6H), 1.37 (d, *J* = 7.1 Hz, 3H), 1.00 (2d, *J* = 6.7 *Hz*, 6H). LC/MS (*m/z*) 635.4 [M+H], Tr = 5.01 min.

(*E*)-(2*R*,5*S*,11*S*,14*S*,17*R*,18*R*)-11-(3-Hydroxy-benzyl)-14-isopropyl-18-methoxy-2,17-dimethyl-3-oxa-9,12,15,28-tetraaza-tricyclo[21.3.1.1^{5,9}]octacosa-1(26),21,23(27),24-tetraene-4,10,13,16-tetraone (7)

Hoveyda-Grubbs II catalyst (25 mg, 0.04 mmol) was added to a solution of **27** (318 mg, 0.402 mmol) in 1,2-dichloroethane (150 mL) and the reaction was heated at reflux under nitrogen for 3 h. The reaction was cooled and silica was added. The solvent was evaporated and the resultant residue purified by silica gel chromatography eluting with *iso*-hexane/ethyl acetate 1:2 to afford the macrocycle (214 mg, 70%) as a brown foam which was dissolved in tetrahydrofuran (10 mL) and tetrabutylammonium fluoride (1.0 M solution in THF, 0.45 mL, 0.45 mmol) was added. The reaction was stirred at room temperature for 1 h. Silica was added and the solvent was evaporated. The residue was purified by silica gel chromatography eluting with a stepwise gradient of *iso*-hexane/ethyl acetate 1:2 to 1:3 by preparative TLC eluting with *iso*-hexane/ethyl acetate 1:3 to afford the title product (115 mg, 63%) as a colorless solid. ^{1}H NMR (300 MHz, CD_3CN) δ 8.25 (s, 1H), 7.34 (d, *J* = 8.0 Hz, 1H), 7.27–7.19 (m, 3H), 7.12–7.01 (m, 3H), 6.98–6.91 (m, 2H), 6.69–6.60 (m, 1H), 6.10–5.98 (m, 1H), 5.81–5.67 (m, 2H), 5.48 (dt, *J* = 9.2, 6.2 Hz, 1H), 4.36 (*br* d, *J* = 13.4 Hz, 1H), 4.20 (t, *J* = 8.5 Hz, 1H), 3.97 (d, *J* = 12.3 Hz, 1H), 3.65 (dt, *J* = 11.8, 3.1 Hz, 1H), 3.45 (s, 3H), 3.38–3.28 (m, 1H), 2.89 (d, *J* = 6.3 Hz, 2H), 2.73–2.58 (m, 2H), 2.10–1.60 (m, 9H), 1.57 (d, *J* = 6.7 Hz, 3H), 1.31 (d, *J* = 7.4 Hz, 3H), 0.97 (d, *J* = 6.7 Hz, 3H), 0.96 (d, *J* = 6.9 Hz, 3H). LC/MS (*m/z*) 649.3 [M+H], Tr = 4.96 min.

(*E*)-(2*R*,5*S*,11*S*,14*S*,17*R*,18*R*)-14-Isopropyl-18-methoxy-2,11,17-trimethyl-3-oxa-9,12,15,28-tetraaza-tricyclo[21.3.1.1^{5,9}]octacosa-1(27),21,23,25-tetraene-4,10,13,16-tetraone (8)

A solution of **32** (195 mg, 0.334 mmol) in 1,2-dichloroethane (110 mL) was treated with Hoveyda-Grubbs II catalyst (20.9 mg, 0.033 mmol). After stirring at reflux for 40 min, the reaction was cooled to room temperature, the volatiles were removed *in vacuo* and the residue was purified by silica gel chromatography using a 25 g Isolute cartridge eluting with a continuous gradient of *iso*-hexane/ethyl acetate 1:1 to 0:1 to provide the title compound (52.5 mg, 28%) as a white solid along with mixed fractions (33.3 mg). ^{1}H NMR (300 MHz, d_6-DMSO) δ 8.04 (d, J = 7.6 Hz, 1H), 7.37–7.13 (m, 4H), 7.06 (d, J = 8.9 Hz, 1H), 6.34–6.14 (m, 2H), 5.81 (q, J = 6.7 Hz, 1H), 5.25–5.10 (m, 2H), 4.10 (*app* t, J = 8.7 Hz, 1H), 3.53 (*app* t, J = 9.4 Hz, 1H), 3.31 (s, 3H), 2.93–2.77 (m, 1H), 2.62 (dd, J = 7.1, 3.3 Hz, 1H), 2.29–2.15 (m, 1H), 2.07–1.58 (m, 4H), 1.75–1.51 (m, 4H), 1.51–1.42 (m, 4H), 1.30 (d, J = 7.1 Hz, 3H), 1.11 (d, J = 7.1 Hz, 3H), 0.87 (d, J = 6.7 Hz, 3H), 0.82 (d, J = 6.7 Hz, 3H). LC/MS (*m/z*) 557.3 [M+H], 579.3 [M+Na], Tr = 5.20 min.

(1^3*S*,4*R*,14*S*,17S,*E*)-14-Isopropyl-4,17-dimethyl-1^1,1^2,1^3,1^4,1^5,1^6-hexahydro-3-oxa-13,16-diaza-1(3,1)-pyridazina-5(1,3)-benzenacyclooctadecaphan-6-ene-2,12,15,18-tetraone (9)

A solution of **33** (330 mg, 0.61 mmol) in 1,2-dichloroethane (200 mL) was treated with Hoveyda-Grubbs II catalyst (52 mg, 0.06 mmol). After stirring at reflux for 60 min under argon atmosphere, the reaction was cooled down to room temperature, the volatiles were removed *in vacuo* and the residue was purified by silica gel chromatography using a gradient from 20 to 80% ethyl acetate + methanol (4/1) in hexane to provide the title compound (70 mg, 22%) as a white solid. ^{1}H NMR (400 MHz, DMSO-d_6) δ 7.94–7.86 (m, 2H), 7.36–7.21 (m, 3H), 7.16 (dt, J = 7.6,

1.5 Hz, 1H), 6.36–6.12 (m, 2H), 5.81 (q, *J* = 6.5 Hz, 1H), 5.19 (d, *J* = 11.3 Hz, 1H), 5.17–5.05 (m, 1H), 4.18–4.05 (m, 1H), 3.52 (td, *J* = 11.0, 2.9 Hz, 1H), 2.85–2.71 (m, 1H), 2.29 (ddd, *J* = 13.2, 11.4, 4.0 Hz, 1H), 2.22–2.09 (m, 1H), 2.09–1.91 (m, 2H), 1.91–1.80 (m, 2H), 1.75–1.59 (m, 3H), 1.61–1.40 (m, 4H), 1.37–1.22 (m, 4H), 0.84 (dd, *J* = 7.1, 7.1 Hz, 6H). LC/MS (*m*/*z*) 513.2 [M + H].

2,2-Dimethyl-propionic acid (*E*)-(2*S*,3*S*,4*S*,5*S*)-3,5-dimethoxy-2,4-dimethyl-oct-6-enyl ester (11)

To 18-crown-6 (3.8 g, 14.4 mmol) in anhydrous tetrahydrofuran (90 mL) at 0 °C and under an atmosphere of nitrogen was added potassium hydride (30 wt% dispersion in mineral oil, 6.7 g, 50.4 mmol) and the suspension was stirred for 5 min. Iodomethane (2.5 mL, 40.3 mmol) was then added at 0 °C and the reaction stirred for an additional 5 min. A solution of **10** (12 g, 7.2 mmol, prepared as described previously[39]) in anhydrous tetrahydrofuran (40 mL) was added dropwise and the reaction was allowed to warm to room temperature and was stirred overnight. The reaction was carefully quenched with saturated ammonium chloride and extracted with diethyl ether (2×). The combined organic layers were dried over anhydrous magnesium sulfate, filtered, and concentrated *in vacuo*. The product was purified by silica gel chromatography eluting with *iso*-hexane/ethyl acetate 25:1 to afford ((*E*)-(2*S*,3*S*,4*S*,5*S*)-3,5-dimethoxy-2,4-dimethyl-oct-6-enyloxymethyl)-benzene (2.0 g, 91%) as a clear oil. ^{1}H NMR (300 MHz, $CDCl_3$) δ 7.40-7.29 (m, 5H), 5.66 (dq, *J* = 15.3, 6.4 Hz, 1H), 5.21 (ddd, *J* = 15.3, 8.8, 1.6 Hz, 1H), 4.54 (s, 2H), 3.61 (dd, *J* = 8.8, 3.3 Hz, 1H), 3.53–3.46 (m, 2H), 3.40 (s, 3H), 3.36 (t, *J* = 9.7 Hz, 1H), 3.23 (s, 3H), 1.98–1.87 (m, 1H), 1.77 (dd, *J* = 6.4, 1.6 Hz, 3H), 1.73–1.65 (m, 1H), 0.95 (d, *J* = 6.9 Hz, 3H), 0.75 (d, *J* = 6.9 Hz, 3H).

To ((*E*)-(2*S*,3*S*,4*S*,5*S*)-3,5-dimethoxy-2,4-dimethyl-oct-6-enyloxymethyl)-benzene (5.5 g, 18.0 mmol) in anhydrous tetrahydrofuran (180 mL) at −78 °C and under an atmosphere of nitrogen, was slowly added freshly prepared lithium di-*tert*-butylbiphenyl solution until a dark green color persisted. The temperature was maintained below −70 °C during the addition. The reaction was quenched with saturated ammonium chloride, allowed to warm to room temperature and extracted with diethyl ether (2×). The combined organic layers were dried over anhydrous magnesium sulfate, filtered, and concentrated *in vacuo*. The product was purified by silica gel chromatography eluting with a stepwise gradient of *iso*-hexane/ethyl acetate 50:1 to 1:1 to afford (*E*)-(2*S*,3*S*,4*S*,5*S*)-3,5-dimethoxy-2,4-dimethyl-oct-6-en-1-ol (3.6 g, 93%) as a clear oil. ^{1}H NMR (300 MHz, $CDCl_3$) δ 5.66 (dq, J = 15.2, 6.4 Hz, 1H), 5.19 (dd, J = 15.2, 8.8 Hz, 1H), 3.75–3.52 (m, 3H), 3.49 (s, 3H), 3.31 (t, J = 9.1 Hz, 1H), 3.24 (s, 3H), 2.82 (dd, J = 8.2, 2.9 Hz, 1H), 1.96–1.88 (m, 1H), 1.77 (d, J = 6.4 Hz, 3H), 1.71–1.63 (m, 1H), 0.84 (d, J = 6.9 Hz, 3H), 0.79 (d, J = 7.1 Hz, 3H).

To (*E*)-(2*S*,3*S*,4*S*,5*S*)-3,5-dimethoxy-2,4-dimethyl-oct-6-en-1-ol (1.5 g, 6.94 mmol) in anhydrous pyridine (20 mL) at 0 °C and under an atmosphere of nitrogen was added pivaloyl chloride (1.33 mL, 10.7 mmol). The reaction was warmed to room temperature and stirred for 2 h, after which it was quenched with saturated ammonium chloride and extracted with dichloromethane (2×). The combined organic layers were filtered through a hydrophobic frit and concentrated *in vacuo*. The product was purified by silica gel chromatography eluting with a stepwise gradient of *iso*-hexane/ethyl acetate 20:1 to 1:1 to afford the title compound (2.0 g, 100%) as a clear oil. ^{1}H NMR (300 MHz, $CDCl_3$) δ 5.67 (dq, J = 15.3, 6.6 Hz, 1H), 5.26–5.15 (m, 1H), 4.23 (dd, J = 10.6, 3.3 Hz, 1H), 4.1 (dd, J = 10.6, 6.0 Hz, 1H), 3.52 (dd, J = 10.0, 2.0 Hz, 1H), 3.42 (s, 3H),

3.34 (t, *J* = 9.3 Hz, 1H), 3.25 (s, 3H), 2.03–1.88 (m, 1H), 1.78 (dd, *J* = 6.4 Hz, 1.5 Hz, 3H), 1.74–1.62 (m, 1H), 1.24 (s, 9H), 0.90 (d, *J* = 7.1 Hz, 3H), 0.76 (d, *J* = 7.1 Hz, 3H).

2,2-Dimethyl-propionic acid (*E*)-(2*S*,3*S*,4*S*,5*S*)-3,5-dimethoxy-2,4-dimethyl-nona-6,8-dienyl ester (12)

To **11** (2.0 g, 6.94 mmol) in anhydrous dichloromethane (60 mL) at −78 °C, ozone was bubbled through until a pale blue color persisted. Nitrogen was then bubbled through until the solution turned colorless. Triphenylphosphine (2.7 g, 10.4 mmol) was added and the reaction was warmed to room temperature and stirred overnight. The reaction was concentrated *in vacuo* and the product was purified by silica gel chromatography eluting with a stepwise gradient of *iso*-hexane/ethyl acetate 20:1 to 4:1 to afford 2,2-dimethyl-propionic acid (2*S*,3*S*,4*R*,5*R*)-3,5-dimethoxy-2,4-dimethyl-6-oxo-hexyl ester (1.62 g, 81%) as a yellow oil. ^{1}H NMR (300 MHz, $CDCl_3$) δ 9.51 (d, *J* = 4.1 Hz, 1H), 4.14 (dd, *J* = 10.8, 3.3 Hz, 1H), 4.00 (dd, *J* = 10.8, 5.9 Hz, 1H), 3.36–3.29 (m, 2H), 3.33 (s, 3H), 3.32 (s, 3H), 1.97–1.87 (m, 2H), 1.20 (s, 9H), 0.84 (d, *J* = 7.0 Hz, 3H), 0.78 (d, *J* = 7.0 Hz, 3H).

To diethylallylphosphonate (1.86 g, 10.4 mmol) in anhydrous tetrahydrofuran (25 mL), at –78 °C and under an atmosphere of nitrogen, was slowly added *n*-butyllithium (2.5 M in hexanes, 4.2 mL, 10.4 mmol) maintaining the temperature below −78 °C. The reaction was stirred at –78 °C for 30 min after which a solution of 2,2-dimethyl-propionic acid (2*S*,3*S*,4*R*,5*R*)-3,5-dimethoxy-2,4-dimethyl-6-oxo-hexyl ester (2.0 g, 6.9 mmol) and 1,3-dimethyltetrahydropyrimidin-2(1*H*)-one (freshly distilled over calcium hydride, 1.7 mL, 13.9 mmol) in anhydrous tetrahydrofuran (5 mL) was added. The reaction was allowed to stir at −78 °C for 1 h and then warmed to room temperature and stirred overnight. The reaction was diluted with saturated ammonium chloride

and extracted with dichloromethane (2×). The combined organic layers were filtered through a hydrophobic frit and concentrated *in vacuo*. The product was purified by silica gel chromatography eluting with *iso*-hexane/ethyl acetate 20/1 to afford the title compound (1.3 g, 60%) as a clear oil. ^{1}H NMR (300 MHz, $CDCl_3$) δ 6.41 (dt, J = 16.8, 10.2 Hz, 1H), 6.24 (dd, J = 15.2, 10.4 Hz, 1H), 5.47 (dd, J = 15.2, 8.6 Hz, 1H), 5.25 (dd, J = 16.8, 1.5 Hz, 1H), 5.13 (dd, J = 9.7, 1.5 Hz, 1H), 4.23 (dd, J = 10.6, 3.3 Hz, 1H), 4.01 (dd, J = 10.6, 6.0 Hz, 1H), 3.52 (dd, J = 10.0, 2.0 Hz, 1H), 3.43 (s, 3H), 3.48–3.39 (m, 1H), 3.27 (s, 3H), 2.03–1.89 (m, 1H), 1.79–1.66 (m, 1H), 1.24 (s, 9H), 0.90 (d, J = 6.9 Hz, 3H), 0.77 (d, J = 7.1 Hz, 3H).

(*E*)-(2*R*,3*R*,4*S*,5*S*)-3,5-Dimethoxy-2,4-dimethyl-nona-6,8-dienoic acid (13)

To **12** (1.3 g, 4.2 mmol) in anhydrous methanol (10 mL) at room temperature and under an atmosphere of nitrogen was added sodium methoxide (30wt% in methanol, 3.7 mL, 20.8 mmol). The reaction was stirred overnight. More sodium methoxide (30wt% in methanol, 3.7 mL, 20.8 mmol) was added and the reaction was stirred for 1 h. The reaction was quenched with saturated ammonium chloride and extracted with dichloromethane (3×). The combined organic layers were dried by passing through a hydrophobic frit and concentrated *in vacuo*. The product was purified by silica gel chromatography eluting with a stepwise gradient of *iso*-hexane/ethyl acetate 10:1 to 2:1 to afford (*E*)-(2*S*,3*S*,4*S*,5*S*)-3,5-dimethoxy-2,4-dimethyl-nona-6,8-dien-1-ol (2.0 g, 100%) as a clear oil. ^{1}H NMR (300 MHz, $CDCl_3$) δ 6.40 (dt, J = 16.8, 10.2 Hz, 1H), 6.23 (dd, J = 15.2, 10.4 Hz, 1H), 5.46 (dd, J = 15.2, 8.4 Hz, 1H), 5.26 (dd, J = 17.0, 1.6 Hz, 1H), 5.14 (dd, J = 10.2, 1.6 Hz, 1H), 3.77–3.53 (m, 3H), 3.51 (s, 3H), 3.42 (t, J = 9.3 Hz, 1H), 3.27 (s, 3H), 2.75 (dd, J = 8.4, 3.1 Hz, 1H), 1.99–1.82 (m, 1H), 1.77–1.65 (m, 1H), 0.85 (d, J = 7.1 Hz, 3H), 0.80 (d, J = 7.1 Hz, 3H).

To (*E*)-(2*S*,3*S*,4*S*,5*S*)-3,5-dimethoxy-2,4-dimethyl-nona-6,8-dien-1-ol (1.3 g, 5.70 mmol) in anhydrous dichloromethane (58 mL) at room temperature and under an atmosphere of nitrogen was added activated 4 Å molecular sieves (1.3 g), *N*-methylmorpholine-*N*-oxide (2.0 g, 17.1 mmol) and tetrapropylammonium perruthenate (100 mg, 0.29 mmol). The reaction was stirred for 3 h and filtered through a silica gel pad, and the pad was washed with diethyl ether. The filtrate was concentrated *in vacuo* to afford (*E*)-(2*R*,3*R*,4*S*,5*S*)-3,5-dimethoxy-2,4-dimethyl-nona-6,8-dienal (1.2 g, 93%) as a clear oil. ^{1}H NMR (300 MHz, $CDCl_3$) δ 9.83 (d, J = 2.7 Hz, 1H), 6.40 (dt, J = 16.8, 10.2 Hz, 1H), 6.24 (dd, J = 15.2, 10.6 Hz, 1H), 5.45 (dd, J = 15.2, 8.8 Hz, 1H), 5.26 (dd, J = 16.4, 1.3 Hz, 1H), 5.14 (dd, J = 10.2, 1.6 Hz, 1H), 3.87 (dd, J = 9.1, 2.4 Hz, 1H), 3.48–3.40 (m, 1H), 3.43 (s, 3H), 3.26 (s, 3H), 2.70–2.55 (m, 1H), 1.78–1.61 (m, 1H), 1.00 (d, J = 7.1 Hz, 3H), 0.82 (d, J = 7.1 Hz, 3H).

To (*E*)-(2*R*,3*R*,4*S*,5*S*)-3,5-dimethoxy-2,4-dimethyl-nona-6,8-dienal (1.2 g, 5.3 mmol) in *tert*-butanol (24 mL) and 2-methyl-2-butene (5.6 mL, 53.1 mmol) at room temperature, was added a solution of sodium chlorite (2.4 g, 26.5 mmol) and sodium dihydrogenphosphate (1.5 g, 10.6 mmol) in water (5 mL). The reaction was stirred vigorously for 1.5 h, after which brine (10 mL) was added and the reaction acidified to pH 5 with hydrochloric acid (2 M). The aqueous was extracted with dichloromethane (3×), the organics were combined, filtered through a hydrophobic frit and concentrated *in vacuo*. The oily residue was left on a vacuum pump overnight to afford the title product (1.02 g, 79%) as an orange solid. ^{1}H NMR (300 MHz, $CDCl_3$) δ 6.39 (dt, J = 16.7, 10.3 Hz, 1H), 6.23 (dd, J = 14.9, 10.5 Hz, 1H), 5.45 (dd, J = 14.9, 8.7 Hz, 1H), 5.26 (d, J = 16.3 Hz, 1H), 5.14 (d, J = 10.3 Hz, 1H), 3.91 (dd, J = 9.4, 1.8 Hz, 1H), 3.46 (s, 3H), 3.52–3.37 (m, 1H), 3.26 (s, 3H), 2.74–2.58 (m, 1H), 1.80–1.64 (m, 1H), 1.13 (d, J = 7.1 Hz, 3H), 0.78 (d, J = 7.1 Hz, 3H).

(*S*)-1-{(*S*)-2-((*S*)-2-*tert*-Butoxycarbonylamino-3-methyl-butyrylamino)-3-[3-(*tert*-butyl-dimethyl-silanyloxy)-phenyl]-propionyl}-hexahydro-pyridazine-3-carboxylic acid but-3-enyl ester (15)

A solution of **14** (1.891 g, 2.562 mmol, prepared as described previously[27]) in tetrahydrofuran (50 mL) was successively treated with zinc powder (3.685 g, 56.368 mmol) and a solution of ammonium acetate (2.962 g, 38.430 mmol) in water (10 mL). After stirring for 24 h at room temperature, the mixture was filtered through a pad of Celite and rinsed with a dilute solution of potassium hydrogensulfate (pH 4). The aqueous layer was extracted with ethyl acetate (3 × 50 mL) and the organics were combined, dried over anhydrous sodium sulfate and filtered. The volatiles were removed *in vacuo* and the residual acetic acid was azeotroped off with toluene (3 × 50 mL) to provide (*S*)-1-{(*S*)-2-((*S*)-2-*tert*-butoxycarbonylamino-3-methyl-butyrylamino)-3-[3-(*tert*-butyl-dimethyl-silanyloxy)-phenyl]-propionyl}-hexahydro-pyridazine-3-carboxylic acid as a white solid which was then suspended in anhydrous toluene (20 mL). Upon the addition of triethylamine (540 μL, 3.843 mmol), the mixture became clear. The mixture was subsequently treated with 2,4,6-trichlorobenzoyl chloride (480 μL, 3.074 mmol). After stirring for 50 min at room temperature, a solution of allyl alcohol (330 μL, 3.843 mmol) and 4-dimethylaminopyridine (469 mg, 3.843 mmol) in toluene (20 mL) was added. After stirring overnight at room temperature, the volatiles were removed *in vacuo* and the residue was purified by silica gel chromatography using a 50 g Isolute cartridge eluting with a continuous gradient of *iso*-hexane/ethyl acetate 1:0 to 1:2 to provide the title compound (85 mg, 14% over 2 steps) as a white solid. ^{1}H NMR (300 MHz, $CDCl_3$) δ 7.13 (*app* t, J = 7.5 Hz, 1H), 6.81 (d, J = 7.5 Hz, 1H), 6.74–6.64 (m, 2H), 6.48 (d, J = 8.4 Hz, 1H), 5.90–5.68 (m, 2H), 5.18–5.08 (m, 2H), 5.08–5.01 (m, 1H), 4.34–4.25 (*br* d, J = 13.9 Hz, 1H), 4.18 (*app* dp, J = 6.8, 4.4 Hz, 2H), 4.00–3.90 (m,

1H), 3.52 (d, *J* = 11.0 Hz, 1H), 2.93 (qd, *J* = 15.5, 6.0 Hz, 2H), 2.81–2.70 (m, 1H), 2.59–2.48 (m, 1H), 2.41 (*app* q, *J* = 6.8 Hz, 2H), 2.20–2.06 (m, 1H), 1.88–1.73 (m, 2H), 1.57–1.49 (m, 2H), 1.46 (s, 9H), 0.99 (s, 9H), 0.94 (d, *J* = 6.8 Hz, 3H), 0.88 (d, *J* = 6.8 Hz, 3H), 0.20 (s, 6H). LC/MS (*m/z*) 661.6 [M+H], 683.5 [M+Na], Tr = 5.79 min.

(*S*)-1-{(*S*)-3-[3-(*tert*-Butyl-dimethyl-silanyloxy)-phenyl]-2-[(*S*)-2-((*E*)-(2*R*,3*R*,4*S*,5*S*)-3,5-dimethoxy-2,4-dimethyl-nona-6,8-dienoylamino)-3-methyl-butyrylamino]-propionyl}-hexahydro-pyridazine-3-carboxylic acid but-3-enyl ester (16)

A cooled (0 °C) solution of **15** (328 mg, 0.500 mmol) in anhydrous dichloromethane (15 mL) was treated with trimethylsilyl trifluoromethane sulfonate (140 μL, 0.750 mmol). After 1.5 h at 0 °C, *N,N*-diisopropylethylamine (0.3 mL, 2.0 mmol) was added and the volatiles were removed *in vacuo* to provide crude (*S*)-1-{(*S*)-2-((*S*)-2-amino-3-methyl-butyrylamino)-3-[3-(*tert*-butyl-dimethyl-silanyloxy)-phenyl]-propionyl}-hexahydro-pyridazine-3-carboxylic acid but-3-enyl ester as a white solid which was used without further purification.

A cooled (0 °C) solution of **13** (100 mg, 0.413 mmol) in anhydrous *N,N*-dimethylformamide (1 mL) was successively treated with *N,N*-diisopropylethylamine (290 μL, 1.652 mmol) and a solution of 2-(1H-7-azabenzotriazol-1-yl)-1,1,3,3-tetramethyl uronium hexafluorophosphate methanaminium (188 mg, 0.496 mmol) in *N,N*-dimethylformamide (1 mL). After 40 min at 0 °C, the reaction mixture was treated with a solution of freshly prepared (*S*)-1-{(*S*)-2-((*S*)-2-amino-3-methyl-butyrylamino)-3-[3-(*tert*-butyl-dimethyl-silanyloxy)-phenyl]-propionyl}-hexahydro-pyridazine-3-carboxylic acid but-3-enyl ester in *N,N*-dimethylformamide (2 mL). The green solution was allowed to warm overnight to room temperature and then quenched with pH 7 buffer (10 mL). The aqueous layer was extracted with dichloromethane (3 × 10 mL) and the

organics were combined, dried over anhydrous sodium sulfate, filtered, and the volatiles were removed *in vacuo*. The residual *N,N*-dimethylformamide was azeotroped off with toluene (2 × 30 mL) and the solid residue was purified by silica gel chromatography using a 25 g Isolute cartridge eluting with a continuous gradient of *iso*-hexane/ethyl acetate 1:0 to 1:1 to provide the title compound (229 mg, 70%) as a white solid. ^{1}H NMR (300 MHz, $CDCl_3$) δ 7.12 (*app* t, J = 8.2 Hz, 1H), 6.80 (d, J = 8.2 Hz, 1H), 6.74–6.63 (m, 2H), 6.50–6.32 (m, 2H), 6.27 (s, 1H), 6.25–6.16 (m, 1H), 5.90–5.67 (m, 2H), 5.47 (dd, J = 15.0, 8.8 Hz, 1H), 5.25 (d, J = 16.1 Hz, 1H), 5.18–5.08 (m, 3H), 4.29 (dd, J = 7.9, 6.0 Hz, 2H), 4.18 (*app* dp, J = 6.6, 5.3 Hz, 2H), 3.87 (dd, J = 9.1, 2.2 Hz, 1H), 3.53 (d, J = 11.1 Hz, 1H), 3.42 (*app* q, J = 9.3 Hz, 1H), 3.40 (s, 3H), 3.25 (s, 3H), 2.99–2.85 (m, 2H), 2.78–2.69 (m, 1H), 2.62–2.50 (m, 1H), 2.46–2.32 (m, 3H), 2.22–2.08 (m, 1H), 1.89–1.67 (m, 2H), 1.53–1.40 (m, 1H), 1.31–1.25 (m, 2H), 1.07 (d, J = 7.0 Hz, 3H), 0.99 (s, 9H), 0.98 (d, J = 6.8 Hz, 3H), 0.96 (d, J = 6.8 Hz, 3H), 0.77 (d, J = 7.1 Hz, 3H), 0.19 (s, 6H). LC/MS (*m/z*) 785.6 [M+H], 807.6 [M+Na], Tr = 5.97 min.

(2*R*,3*R*)-1-((1*R*,5*S*)-10,10-Dimethyl-3,3-dioxo-3λ^6-thia-4-aza-tricyclo[5.2.1.0^{1,5}]dec-4-yl)-3-hydroxy-2-methyl-hept-6-en-1-one (18)

A solution of **17** (3.95 g, 14.55 mmol) in toluene (50 mL) was prepared, then evaporated to dryness. This process was repeated and then the resulting white solid was dissolved in anhydrous dichloromethane (16 mL). A small quantity of calcium hydride was added before adding *tert*-butyldimethylsilyl trifluoromethanesulfonate (3.83 mL, 14.5 mmol) and anhydrous triethylamine (2.33 mL, 16.7 mmol). The reaction mixture was stirred at room temperature under a nitrogen atmosphere for 15 h. The resulting solution was evaporated to yield a thick paste which was dissolved in anhydrous dichloromethane (15 mL) and added dropwise to a cooled (–78 °C)

solution of 4-pentenal (2.69 g, 32.0 mmol) and titanium tetrachloride (1 M in dichloromethane, 32 mL, 32 mmol) in anhydrous dichloromethane (20 mL). The reaction was stirred at –78 °C for 30 min before diluting with saturated aqueous ammonium chloride solution (100 mL). The layers were separated and the aqueous layer was extracted with dichloromethane (2 × 50 mL). The combined extracts were dried over anhydrous sodium sulfate, filtered, and evaporated to give a brown gum which was purified by silica gel chromatography eluting with *iso*-hexane/ethyl acetate 4:1 to yield the title compound (3.09 g, 60%) as a colorless gum. ^{1}H NMR (300 MHz, $CDCl_3$) δ 5.90–5.74 (m, 1H), δ5.00–4.94 (m, 2H), 3.91 (dd, J = 7.6, 5.1 Hz, 1H), 3.67 (*br* s, 1H), 3.50 (ABq, $\Delta\delta_{AB}$ = 0.06, J_{AB} = 13.8 Hz, 2H), 3.26–3.15 (m, 1H), 2.53–2.08 (m, 5H), 2.01–1.84 (m, 3H), 1.76–1.63 (m, 1H), 1.55–1.31 (m, 3H), 1.25 (d, J = 6.7 Hz, 3H), 1.19 (s, 3H), 0.99 (s, 3H). LC/MS (*m/z*) 356.2 [M+H], Tr = 3.41 min.

(2*R*,3*R*)-3-Methoxy-2-methylhept-6-enoic acid (19)

A solution of **18** (250 mg, 0.703 mmol) in anhydrous dichloromethane (7 mL) was prepared and a solution of *N,N,N′,N′*-tetramethyl-1,8-naphthalenediamine (452 mg, 0.703 mmol) in anhydrous dichloromethane (7 mL) was added. Trimethyloxonium tetrafluoroborate (208 mg, 1.406 mmol) was then added. The reaction mixture was stirred at room temperature for 15 h. The reaction mixture was then treated with methanol (1 mL), hydrochloric acid (2 M, 20 mL) and saturated brine (20 mL). The aqueous layer was extracted with ethyl acetate (3 × 15 mL) and the extracts were dried over anhydrous sodium sulfate, filtered, and evaporated to give a yellow gum. The gum was purified by silica gel chromatography eluting with *iso*-hexane/ethyl acetate 3:1 to give (2*R*,3*R*)-1-((1*R*,5*S*)-10,10-dimethyl-3,3-dioxo-3λ^6-thia-4-aza-tricyclo[5.2.1.0^{1,5}]dec-4-yl)-3-methoxy-2-methyl-hept-6-en-1-one (223 mg, 86%) as a colorless gum. ^{1}H NMR (300 MHz,

$CDCl_3$) δ 5.86–5.70 (m, 1H), 5.06–4.91 (m, 2H), 3.89 (dd, J = 7.4, 5.1 Hz, 1H), 3.56–3.34 (m, 4H), 3.32 (s, 1H), 2.27–2.00 (m, 5H), 1.98–1.81 (m, 4H), 1.60–1.48 (m, 2H), 1.45–1.30 (m, 2H), 1.18 (s, 3H), 1.09 (d, J = 6.7 Hz, 3H), 0.97 (s, 3H). LC/MS (*m/z*) 370.2 [M+H], Tr = 3.69 min.

A solution of lithium hydroxide in water (2 M, 5 mL, 10 mmol) was added to a stirred solution of (2*R*,3*R*)-1-((1*R*,5*S*)-10,10-dimethyl-3,3-dioxo-3λ^6-thia-4-aza-tricyclo[5.2.1.$0^{1,5}$]dec-4-yl)-3-methoxy-2-methyl-hept-6-en-1-one (223 mg, 0.60 mmol) in tetrahydrofuran (15 mL). The stirred mixture was heated to 60 °C for 15 h. The reaction mixture was partially evaporated before adding hydrochloric acid (2 M, 20 mL). The solution was extracted with ethyl acetate (3 × 15 mL). The extracts were dried over anhydrous sodium sulfate, filtered, and evaporated to give a yellow gum (209 mg). The gum was purified by silica gel chromatography eluting with *iso*-hexane/ethyl acetate 3:1 to yield the title compound (68 mg, 66%) as a yellow gum. ^{1}H NMR (300 MHz, $CDCl_3$) δ 5.91–5.76 (m, 1H), 5.10–4.97 (m, 2H), 3.53–3.45 (m, 1H), 3.40 (s, 3H), 2.85–2.74 (m, 1H), 2.23–2.11 (m, 2H), 1.67–1.57 (m, 2H), 1.16 (d, J = 6.9 Hz, 3H).

(*R*)-1-(3-Vinyl-phenyl)-ethanol (21)

Bis(triphenylphosphine)palladium(II) dichloride (360 mg, 0.512 mmol) was added to a degassed solution of **20** (1.03 g, 5.123 mmol) and tributyl(vinyl)tin (1.8 mL, 6.1 5mmol) in toluene (10 mL) under nitrogen and the reaction was stirred at 45 °C for 18 h. Tributyl(vinyl)tin (750 µL, 2.56mmol) and bis(triphenylphosphine)palladium(II) dichloride (180 mg, 0.256 mmol) were added and stirring was continued for 18 h. The reaction was cooled and the solvent was evaporated to afford a residue which was absorbed onto silica. Purification by silica gel chromatography eluting with *iso*-hexane/ethyl acetate 3:1 afforded the title product (675 mg, 89%) as a yellow oil. ^{1}H NMR (300 MHz, $CDCl_3$) δ 7.49 (s, 1H), 7.38–7.29 (m, 3H), 6.75 (dd, J

= 17.6, 10.9 Hz, 1H), 5.80 (d, *J* = 17.6 Hz, 1H), 5.28 (d, *J* = 10.7 Hz, 1H), 4.99–4.87 (m, 1H), 1.81 (d, *J* = 3.1 Hz, 1H), 1.52 (d, *J* = 6.5 Hz, 3H).

(*S*)-1-{(*S*)-2-((*S*)-2-*tert*-Butoxycarbonylamino-3-methyl-butyrylamino)-3-[3-(*tert*-butyl-dimethyl-silanyloxy)-phenyl]-propionyl}-hexahydro-pyridazine-3-carboxylic acid (*E*)-hexa-3,5-dienyl ester (22)

A solution of **14** (2.709 g, 3.669 mmol) in tetrahydrofuran (50 mL) was subsequently treated with zinc powder (5.279 g, 80.727 mmol) and a solution of ammonium acetate (4.242 g, 55.035 mmol) in water (10 mL). After stirring at room temperature for 16 h, the mixture was filtered over Celite. The solid was rinsed with a solution of potassium hydrogen sulfate at pH 5. The aqueous layer was extracted with ethyl acetate (2×). The organics were combined, dried over anhydrous sodium sulfate, filtered, and the volatiles were removed *in vacuo.* Residual acetic acid was azeotroped off with toluene to provide crude (*S*)-1-{(*S*)-2-((*S*)-2-*tert*-butoxycarbonylamino-3-methyl-butyrylamino)-3-[3-(*tert*-butyl-dimethyl-silanyloxy)-phenyl]-propionyl}-hexahydro-pyridazine-3-carboxylic acid (2.456 g) as a white solid which was subsequently suspended in anhydrous toluene (30 mL). This suspension was treated with triethylamine (0.77 mL, 5.503 mmol) and 2,4,6-trichlorobenzoyl chloride (0.69 mL, 4.403 mmol). After stirring for 40 min at room temperature, the mixture was treated with a solution of (*E*)-hexa-3,5-dien-1-ol (432.1 mg, 4.403 mmol, prepared as described previously[45]) and 4-dimethylaminopyridine (672.0 mg, 5.503 mmol) in toluene (5 mL). After stirring at room temperature for 16 h, the volatiles were removed *in vacuo* and the residue was purified by silica gel chromatography using a 50 g Isolute cartridge eluted with a continuous gradient of *iso*-hexane/ethyl acetate 1:0 to 1:1 to afford the title compound (1.77 g, 70%) as a white solid. ^{1}H NMR (300 MHz, $CDCl_3$) δ 7.12 (*app* t, *J* = 7.7 Hz,

1H), 6.81 (d, *J* = 7.7 Hz, 1H), 6.75–6.64 (m, 2H), 6.49 (d, *J* = 8.4 Hz, 1H), 6.33 (dt, *J* = 16.8, 10.4 Hz, 1H), 6.14 (dd, *J* = 15.0, 10.6 Hz, 1H), 5.78–5.57 (m, 2H), 5.15 (d, *J* = 16.1 Hz, 1H), 5.09–4.98 (m, 2H), 4.33–4.23 (m, 1H), 4.22–4.10 (m, 2H), 4.01–3.90 (m, 1H), 3.50 (d, *J* = 11.1 Hz, 1H), 3.03–2.70 (m, 3H), 2.57–2.38 (m, 2H), 2.19–2.06 (m, 1H), 1.86–1.72 (m, 2H), 1.51–1.38 (m, 10H), 1.01–0.79 (m, 17H), 0.19 (s, 6H).

(*S*)-1-{(*S*)-2-((*S*)-2-*tert*-Butoxycarbonylamino-3-methyl-butyrylamino)-3-[3-(*tert*-butyl-dimethyl-silanyloxy)-phenyl]-propionyl}-hexahydro-pyridazine-3-carboxylic acid 3-vinyl-benzyl ester (23)

To 3-vinylbenzaldehyde (2.0 g, 15.1 mmol) in anhydrous methanol (35 mL) at room temperature and under an atmosphere of nitrogen was slowly added sodium borohydride (630 mg, 16.6 mmol) in portions over 15 min. The reaction was stirred for 1 h before being concentrated *in vacuo*. To the residue was added water and the aqueous extracted with dichloromethane (2×). The organic layers were filtered through a hydrophobic frit and concentrated *in vacuo*. The product was purified by silica gel chromatography eluting with *iso*-hexane/ethyl acetate 2:1 to afford (3-vinyl-phenyl)-methanol (2.0 g, 100%) as a clear oil. ^{1}H NMR (300 MHZ, $CDCl_3$) δ 7.49–7.24 (m, 4H), 6.75 (dd, *J* = 17.4, 10.9 Hz, 1H), 5.80 (d, *J* = 17.4 Hz, 1H), 5.29 (d, *J* = 10.9 Hz, 1H), 4.72 (d, *J* = 6.0 Hz, 2H), 1.73 (t, *J* = 6.0 Hz, 1H).

To (3-vinyl-phenyl)-methanol (1.9 g, 14.2 mmol) in tetrahydrofuran (12 mL) at room temperature and under an atmosphere of nitrogen was added **14** (2.6 g, 3.54 mmol), followed by sodium hydride (60wt% in mineral oil, 28 mg, 0.71 mmol). The reaction was warmed to 40 °C for 6 h. After cooling to room temperature, water was added and the aqueous layer was extracted with dichloromethane (2×). The combined organic layers were filtered through a hydrophobic

frit and concentrated *in vacuo*. The product was purified by silica gel chromatography eluting with a stepwise gradient of *iso*-hexane/ethyl acetate 2:1 to 1:2 to afford the title product (1.5 g, 59%) as a viscous clear oil that forms a white foam when placed under vacuum. ^{1}H NMR (300 MHz, $CDCl_3$) δ 7.46–7.32 (m, 3H), 7.30–7.21 (m, 1H), 7.07–6.98 (m, 1H), 6.84–6.77 (m, 1H), 6.77–6.68 (m, 1H), 6.69–6.61 (m, 2H), 6.50 (d, J = 8.0 Hz, 1H), 5.81–5.71 (m, 2H), 5.31 (d, J = 10.7 Hz, 1H), 5.20–5.01 (m, 3H), 4.36–4.23 (m, 1H), 4.02–3.91 (m, 1H), 3.55 (d, J = 11.2 Hz 1H), 3.03–2.81 (m, 2H), 2.80–2.68 (m, 1H), 2.59–2.46 (m, 1H), 2.20–2.07 (m, 1H), 1.90–1.71 (m, 2H), 1.58–1.37 (m, 11H), 1.02–0.79 (m, 15H), 0.18 (s, 6H). LC/MS (*m/z*) 723.5 [M+H], Tr = 5.64 min.

(*S*)-1-{(*S*)-2-((*S*)-2-*tert*-Butoxycarbonylamino-3-methyl-butyrylamino)-3-[3-(*tert*-butyl-dimethyl-silanyloxy)-phenyl]-propionyl}-hexahydro-pyridazine-3-carboxylic acid (*R*)-1-(3-vinyl-phenyl)-ethyl ester (24)

4-Dimethylaminopyridine (165 mg, 1.35 mmol), followed by *N*-(3-dimethylaminopropyl)-*N*′-ethylcarbodiimide hydrochloride (414 mg, 2.16 mmol) was added to a solution of (*S*)-1-{(*S*)-2-((*S*)-2-*tert*-butoxycarbonylamino-3-methyl-butyrylamino)-3-[3-(*tert*-butyl-dimethyl-silanyloxy)-phenyl]-propionyl}-hexahydro-pyridazine-3-carboxylic acid (818 mg, 1.35 mmol, prepared as described in the synthesis of **22**) and **21** (300 mg, 2.025 mmol) in dichloromethane (20 mL) and the reaction was stirred at room temperature for 18 h. The mixture was washed with citric acid, saturated sodium bicarbonate, dried over anhydrous sodium sulfate and the solvent was evaporated to afford a brown oil which was purified by silica gel chromatography eluting with a stepwise gradient of *iso*-hexane/ethyl acetate 2:1 to 1:1 to afford the title compound (537 mg, 54%) as a colorless oil. ^{1}H NMR (300 MHz, $CDCl_3$) δ 7.43–7.32 (m, 3H), 6.93 (t, J = 9.1 Hz,

1H), 6.85–6.65 (m, 3H), 6.64–6.58 (m, 2H), 6.47 (d, *J* = 7.6 Hz, 1H), 5.95–5.65 (m, 3H), 5.34–5.26 (m, 1H), 5.05 (d, *J* = 7.4 Hz, 1H), 4.39–4.29 (m, 1H), 4.00–3.91 (m, 1H), 3.53 (d, *J* = 11.2 Hz, 1H), 3.05–2.80 (m, 3H), 2.79–2.66 (m, 1H), 2.55–2.42 (m, 1H), 2.12 (q, *J* = 5.8 Hz, 1H), 1.95–1.84 (m, 1H), 1.83–1.73 (m, 1H), 1.55 (d, *J* = 6.9 Hz, 3H), 1.46 (s, 9H), 0.98 (s, 9H), 0.94 (d, *J* = 6.7 Hz, 3H), 0.88 (d, *J* = 6.9 Hz, 3H), 0.18 (s, 6H). LC/MS (*m/z*) 737.3 [M+H], Tr = 5.95 min.

(*S*)-1-{(*S*)-3-[3-(*tert*-Butyl-dimethyl-silanyloxy)-phenyl]-2-[(*S*)-2-((2*R*,3*R*)-3-methoxy-2-methyl-hept-6-enoylamino)-3-methyl-butyrylamino]-propionyl}-hexahydro-pyridazine-3-carboxylic acid (*E*)-hexa-3,5-dienyl ester (25)

A solution of **22** (333 mg, 0.485 mmol) in anhydrous dichloromethane (10 mL) was cooled to 0 °C under a nitrogen atmosphere before adding trimethylsilyl trifluoromethanesulfonate (161 µL, 0.727 mmol). The reaction mixture was stirred at 0 °C for 1.5 h before adding *N,N*-diisopropylethylamine (340 µL, 1.94 mmol). The mixture was evaporated to give (*S*)-1-{(*S*)-2-((*S*)-2-amino-3-methyl-butyrylamino)-3-[3-(*tert*-butyl-dimethyl-silanyloxy)-phenyl]-propionyl}-hexahydro-pyridazine-3-carboxylic acid (*E*)-hexa-3,5-dienyl ester as a white solid which was used crude in the next step. LC/MS (*m/z*) 587.3 [M+H], Tr = 4.49 min.

A solution of **19** (83.6 mg, 0.485 mmol) in anhydrous *N,N*-dimethylformamide (4 mL) was cooled to 0 ˚C before adding *N,N*-diisopropylethylamine (340 µL,1.94 mmol) and 2-(1H-7-azabenzotriazol-1-yl)-1,1,3,3-tetramethyl uronium hexafluorophosphate methanaminium (185 mg, 0.485 mmol) The reaction mixture was stirred at 0 ˚C for 20 min before addition of (*S*)-1-{(*S*)-2-((*S*)-2-amino-3-methylbutyryl amino)-3-[3-(*tert*-butyl-dimethyl-silanyloxy)-phenyl]-propionyl}-hexahydro-pyridazine-3-carboxylic acid (*E*)-hexa-3,5-dienyl ester (285 mg, 0.485

mmol) in anhydrous *N,N*-dimethylformamide (4 mL). The reaction mixture was stirred at room temperature for 15 h then was diluted with pH 7 phosphate buffer (0.5 M, 20 mL). The aqueous layer was extracted with ethyl acetate (3 × 20 mL). The combined extracts were washed with brine (3 × 20 mL), dried over anhydrous sodium sulfate, filtered, and evaporated to give a brown gum. The gum was purified by silica gel chromatography eluting with *iso*-hexane/ethyl acetate 2:3 to yield the title compound (133 mg, 37%) as a colorless solid. ^{1}H NMR (300 MHz, $CDCl_3$) 7.11 (t, J = 7.8 Hz, 1H), 6.85–6.78 (d, J = 7.8 Hz, 1H), 6.75–6.64 (m, 2H), 6.59–6.45 (m, 2H), 6.40–6.25 (m, 1H), 6.19–6.08 (m, 1H), 5.90–5.57 (m, 3H), 5.20–4.93 (m, 3H), 4.35–4.09 (m, 5H), 3.54 (d, J = 11.2 Hz, 1H), 3.45–3.31 (m, 4H), 3.01–2.65 (m, 3H), 2.53–2.39 (m, 3H), 2.21–2.08 (m, 3H), 1.85–1.35 (m, 7H), 1.17 (d, J = 7.1 Hz, 3H), 0.97 (s, 9H), 0.96–0.87 (m, 6H), 0.19 (s, 6H). LC/MS (*m/z*) 741.4 [M+H], Tr = 5.72 min.

(*S*)-1-{(*S*)-3-[3-(*tert*-Butyl-dimethyl-silanyloxy)-phenyl]-2-[(*S*)-2-((2*R*,3*R*)-3-methoxy-2-methyl-hept-6-enoylamino)-3-methyl-butyrylamino]-propionyl}-hexahydro-pyridazine-3-carboxylic acid 3-vinyl-benzyl ester (26)

A cooled (0 °C) solution of **23** (400 mg, 0.49 mmol) in anhydrous dichloromethane (20 mL) was treated with trimethylsilyl trifluoromethanesulfonate (0.17 mL, 0.64 mmol). The reaction was stirred for 2 h at 0 °C then quenched by adding *N,N*-diisopropylethylamine (0.45 mL, 2.56 mmol) and concentrated *in vacuo* to yield (*S*)-1-{(*S*)-2-((*S*)-2-amino-3-methyl-butyrylamino)-3-[3-(*tert*-butyl-dimethyl-silanyloxy)-phenyl]-propionyl}-hexahydro-pyridazine-3-carboxylic acid 3-vinyl-benzyl ester as a white solid.

A solution of **19** (80 mg, 0.46 mmol) in anhydrous *N,N*-dimethylformamide (3 mL) was cooled to 0 ˚C under an atmosphere of nitrogen before adding *N,N*-diisopropylethylamine (0.32 mL,

1.86 mmol) and 2-(1H-7-azabenzotriazol-1-yl)-1,1,3,3-tetramethyl uronium hexafluorophosphate methanaminium (177 mg, 0.46 mmol). The reaction was stirred for 0.5 h after which a solution of (*S*)-1-{(*S*)-2-((*S*)-2-amino-3-methyl-butyrylamino)-3-[3-(*tert*-butyl-dimethyl-silanyloxy)-phenyl]-propionyl}-hexahydro-pyridazine-3-carboxylic acid 3-vinyl-benzyl ester in anhydrous *N,N*-dimethylformamide (3 mL) was added. The reaction was warmed to room temperature, stirred for 16 h and quenched with pH 7 buffer. The reaction was extracted with dichloromethane (2×), the organics were filtered through a hydrophobic frit and concentrated *in vacuo*. The product was purified by silica gel chromatography eluting with a stepwise gradient of *iso*-hexane/ethyl acetate 2:1 to 1:1 to afford the title product (280 mg, 78%) as a viscous oil. ^{1}H NMR (300 MHz, $CDCl_3$) δ 7.46–7.32 (m, 3H), 7.30–7.21 (m, 1H), 7.06–6.98 (m, 1H), 6.83–6.62 (m, 4H), 6.55–6.46 (m, 2H), 5.91–5.70 (m, 2H), 5.79 (d, J = 17.6 Hz, 1H), 5.31 (d, J = 10.9 Hz, 1H), 5.15 (s, 2H), 5.05 (dd, J = 17.2, 1.6 Hz, 1H), 4.97 (d, J = 10.0 Hz, 1H), 4.36–4.24 (m, 2H), 3.55 (d, J = 11.4 Hz, 1H), 3.44–3.30 (m, 4H), 3.00–2.81 (m, 2H), 2.80–2.67 (m, 1H), 2.57–2.41 (m, 2H), 2.25–2.09 (m, 3H), 1.90–1.63 (m, 4H), 1.55–1.40 (m, 2H), 1.18 (d, J = 6.9 Hz, 3H), 1.00–0.88 (m, 6H), 0.97 (s, 9H), 0.17 (s, 6H). LC/MS (*m/z*) 777.5 [M+H], Tr = 4.35 min.

(*S*)-1-{(*S*)-3-[3-(*tert*-Butyl-dimethyl-silanyloxy)-phenyl]-2-[(*S*)-2-((2*R*,3*R*)-3-methoxy-2-methyl-hept-6-enoylamino)-3-methyl-butyrylamino]-propionyl}-hexahydro-pyridazine-3-carboxylic acid (*R*)-1-(3-vinyl-phenyl)-ethyl ester (27)

Trimethylsilyltrifluoromethanesulfonate (198 µL, 1.093 mmol) was added dropwise to a solution of **24** (537 mg, 0.729 mmol) in dichloromethane (10 mL) at 0 °C under nitrogen and the reaction was stirred for 1 h. To this was added *N,N*-diisopropylethylamine (508 µL, 2.92 mmol) and the reaction was warmed to room temperature. The volatiles were evaporated to afford (*S*)-1-{(*S*)-2-

((*S*)-2-amino-3-methyl-butyrylamino)-3-[3-(tert-butyl-dimethyl-silanyloxy)-phenyl]-propionyl}-hexahydro-pyridazine-3-carboxylic acid (*R*)-1-(3-vinyl-phenyl)-ethyl ester as a waxy solid which was used without further purification. 1-Hydroxybenzotriazole (123 mg, 0.729 mmol), followed by *N*-(3-dimethylaminopropyl)-*N'*-ethylcarbodiimide hydrochloride (196 mg, 1.02 mmol) was added to a solution of (*S*)-1-{(*S*)-2-((*S*)-2-amino-3-methyl-butyrylamino)-3-[3-(tert-butyl-dimethyl-silanyloxy)-phenyl]-propionyl}-hexahydro-pyridazine-3-carboxylic acid (*R*)-1-(3-vinyl-phenyl)-ethyl ester and **19** (125 mg, 0.729 mmol) in acetonitrile (10 mL) and the reaction was stirred at room temperature for 18 h. The solvent was evaporated and the residue partitioned between water and ethyl acetate. The organic layer was dried over anhydrous sodium sulfate and the solvent evaporated. Purification by silica gel chromatography eluting with *iso*-hexane/ethyl acetate 3:1 afforded the title product (318 mg, 55%) as a colorless foam. ^{1}H NMR (300 MHz, d_6-DMSO) δ 7.72 (d, J = 9.1 Hz, 1H), 7.63–7.54 (m, 1H), 7.47–7.25 (m, 3H), 6.93 (*app* t, J = 7.8 Hz, 1H), 6.81–6.67 (m, 2H), 6.66–6.54 (m, 2H), 5.91–5.70 (m, 3H), 5.48 (q, J = 7.4 Hz, 1H), 5.35–5.16 (m, 2H), 5.00 (dd, J = 17.2, 1.6 Hz, 1H), 4.93 (d, J = 10.0 Hz, 1H), 4.13 (dd, J = 6.9 Hz, 1H), 4.07–3.95 (m, 1H), 3.20 (s, 3H), 3.07–2.78 (m, 3H), 2.75–2.58 (m, 2H), 2.15–1.89 (m, 3H), 1.88–1.79 (m, 1H), 1.73–1.63 (m, 1H), 1.61–1.31 (m, 6H), 0.96–0.84 (m, 12H), 0.77 (d, J = 6.7 Hz, 6H), 0.13 (s, 6H). LC/MS (*m/z*) 791.4 [M+H], Tr = 6.00 min.

(*S*)-1-[(*S*)-2-((*S*)-2-*tert*-Butoxycarbonylamino-3-methylbutyrylamino)-propionyl]-hexahydropyridazine-3-carboxylic acid 2,2,2-trichloroethyl ester (29)

A solution of (*S*)-2-*tert*-butoxycarbonylamino-propionic acid (3.28 g, 17.32 mmol) in acetonitrile (160 mL) was cooled to 0 °C before addition of *N,N*-diisopropylethylamine (12 mL, 69.3 mmol) and 2-(1H-benzotriazole-1-yl)-1,1,3,3-tetramethyluronium hexafluorophosphate (6.57 g, 17.32

mmol). The reaction mixture was stirred at 0 °C for 20 min and a solution of **28** (6.49 g, 17.3 mmol, prepared as described previously[37]) in acetonitrile (80 mL) was added. The reaction was allowed to warm to room temperature and was stirred for 15 h. The reaction mixture was evaporated and the residue was partitioned between ethyl acetate (150 mL) and brine (150 mL). The aqueous layer was extracted with ethyl acetate (50 mL). The organic layers were combined, dried over anhydrous sodium sulfate, filtered, and evaporated to give a dark oil. The oil was purified by silica gel chromatography eluting *iso*-hexane/ethyl acetate 1:1 to yield (*S*)-1-((*S*)-2-*tert*-butoxycarbonylamino-propionyl)-hexahydro-pyridazine-3-carboxylic acid 2,2,2-trichloro-ethyl ester (6.88 g, 92%) as a colorless gum. ^{1}H NMR (300 MHz, $CDCl_3$) δ 5.36 (d, J = 8.0 Hz, 1H), 5.20–5.05 (m, 1H), 4.95 (d, J = 12.0 Hz, 1H), 4.75 (d, J = 12.0 Hz, 1H), 4.43 (d, J = 12.9 Hz, 1H), 3.90–3.75 (m, 1H), 3.75–3.63 (m, 1H), 2.92–2.77 (m, 1H), 2.30–2.12 (m, 1H), 2.03–1.83 (m, 1H), 1.83–1.60 (m, 2H), 1.44 (s, 9H), 1.29 (d, J = 6.9 Hz, 3H).

A solution of (*S*)-1-((*S*)-2-*tert*-butoxycarbonylamino-propionyl)-hexahydro-pyridazine-3-carboxylic acid 2,2,2-trichloro-ethyl ester (6.88 g, 15.9 mmol) in dichloromethane (200 mL) was prepared and trifluoroacetic acid (50 mL) was added. The reaction mixture was stirred at room temperature for 2 h. The solution was evaporated to give a brown oil. Residual trifluoroacetic acid was azeotroped off with toluene (50 mL) and the resultant oil was dried under vacuum to give (S)-1-((S)-2-amino-propionyl)-hexahydro-pyridazine-3-carboxylic acid 2,2,2-trichloro-ethyl ester trifluoroacetic acid salt (7.8 g) as a brown gum.

A solution of ((*S*)-1-carbamoyl-2-methylpropyl)-carbamic acid *tert*-butyl ester (3.628 g, 16.69 mmol) in acetonitrile (300 mL) was cooled to 0 °C before adding *N,N*-diisopropylethylamine (13.8 mL, 79.7 mmol) and 2-(1H-benzotriazole-1-yl)-1,1,3,3-tetramethyluronium hexafluorophosphate (6.33 g, 16.7 mmol). The reaction was stirred at 0 °C for 15 min before

adding a solution of the (*S*)-1-((*S*)-2-amino-propionyl)-hexahydro-pyridazine-3-carboxylic acid 2,2,2-trichloro-ethyl ester trifluoroacetic acid salt (*ca*. 15.9 mmol) in acetonitrile (85 mL). The reaction was stirred at 0 °C for a further 20 min then allowed to warm to room temperature and stirred for 15 h. The reaction mixture was evaporated and the residue was partitioned between ethyl acetate (250 mL) and water (150 mL). The organics were dried over anhydrous sodium sulfate, filtered, and evaporated to give a red oil which was purified by silica gel chromatography eluting with a stepwise gradient of *iso*-hexane/ethyl acetate 7:3 to 1:1 to yield the title compound (8.2 g, 92%) as a pale orange solid. ^{1}H NMR (300 MHz, $CDCl_3$) δ 6.82 (d, J = 7.6 Hz, 1H), 5.40–5.28 (m, 1H), 5.15 (d, J = 8.5 Hz, 1H), 4.97 (d, J = 12.0 Hz, 1H), 4.71 (d, J = 12.0 Hz, 1H), 4.34 (d, J = 12.5 Hz, 1H), 4.05–3.78 (m, 2H), 3.78–3.65 (m, 1H), 2.92 (*br* s, 1H), 2.25–2.05 (m, 2H), 2.00–1.85 (m, 1H), 1.84–1.65 (m, 2H), 1.46 (s, 9H), 1.33 (d, J = 6.7 Hz, 3H), 0.96 (d, J = 6.9 Hz, 3H), 0.90 (d, J = 6.9 Hz, 3H). LC/MS (*m/z*) 531.04 [M+H], Tr = 3.75 min.

(*S*)-1-{(*S*)-2-[(*S*)-2-((2R,3*R*)-3-Methoxy-2-methyl-hept-6-enoylamino)-3-methyl-butyrylamino]-propionyl}-hexahydro-pyridazine-3-carboxylic acid 2,2,2-trichloro-ethyl ester (30)

A solution of **29** (316 mg, 0.59 mmol) in anhydrous dichloromethane (10 mL) was cooled to 0 °C under a nitrogen atmosphere before adding trimethylsilyl trifluoromethanesulfonate (160 µL, 0.885 mmol). The reaction mixture was stirred at 0 °C for 2 h before adding *N,N*-diisopropylethylamine (413 µl, 2.36 mmol). The mixture was evaporated to afford (*S*)-1-[(*S*)-2-((*S*)-2-amino-3-methyl-butyrylamino)-propionyl]-hexahydro-pyridazine-3-carboxylic acid 2,2,2-trichloroethyl ester which was combined with **19** (162 mg, 0.94 mmol.) and dissolved in acetonitrile (13 mL). 1-Ethyl-3-(3-dimethylaminopropyl)carbodiimide (250 mg, 1.32 mmol) and

1-hydroxybenzotriazole (220 mg, 1.32 mmol) were added. The reaction was stirred at room temperature for 15 h then evaporated to give a yellow oil. The oil was purified by silica gel chromatography eluting with ethyl acetate to give the title compound (425 mg, 77%) as a white solid. ^{1}H NMR (300 MHz, CD_3CN) δ 6.99 (d, J = 7.3 Hz, 1H), 6.66 (d, J = 8.7 Hz, 1H), 5.95–5.80 (m, 1H), 5.27–5.15 (m, 1H), 5.11–4.93 (m, 2H), 5.00 (d, J = 12.3 Hz, 1H), 4.80 (d, J = 12.3 Hz, 1H), 4.40 (d, J = 9.1 Hz, 1H), 4.25–4.16 (m, 1H), 3.86–3.72 (m, 1H), 3.40–3.33 (m, 1H), 2.80–2.60 (m, 1H), 2.20–2.01 (m, 4H), 1.90–1.76 (m, 2H), 1.75–1.60 (m, 2H), 1.60–1.45 (m, 1H), 1.33 (d, J = 6.7 Hz, 1H), 1.23 (d, J = 6.7 Hz, 3H), 1.06 (d, J = 7.1 Hz, 3H), 0.96–0.86 (m, 6H). LC/MS (*m/z*) 585.1 [M+H], Tr = 5.48 min.

2,2,2-Trichloroethyl (*S*)-1-(hept-6-enoyl-*L*-valyl-*L*-alanyl)hexahydropyridazine-3-carboxylate (31)

A solution of **29** (1064 mg, 2 mmol) in anhydrous dichloromethane (30 mL) was cooled in an ice water bath. Trimethylsilyl trifluoromethanesulfonate (666 mg, 3 mmol) was added dropwise at 0 °C under argon, and the resulting solution was stirred at room temperature for 30 min. The reaction mixture was evaporated to dryness and the resulting crude residue (LC/MS (*m*/*z*) 431 [M+H]) was dissolved in dry acetonitrile (25 mL) under argon. The reaction mixture was stirred at 0 °C, and hept-6-enoic acid (281 mg, 2.2 mmol) and *N,N*-diisopropylethylamine (1034 mg, 8 mmol) were added followed by 2-(1*H*-7-azabenzotriazol-1-yl)-1,1,3,3-tetramethyl uronium hexafluorophosphate methanaminium (1065 mg, 2.8 mmol). The reaction mixture was stirred at room temperature for 48 h. The solvent was evaporated, the residue was dissolved in ethyl acetate (200 mL) and the solution was washed twice with 20% water solution of citric acid (150 mL), water (150 mL) and brine (150 mL), dried over $MgSO_4$, filtered, and evaporated. The

residue was purified by silica gel chromatography (gradient from 0 to 40% ethyl acetate + methanol (4/1) in hexane) to afford the title compound (817 mg, 75%) as a white solid. ^{1}H NMR (400 MHz, CD_3OD): δ 8.05–7.87 (m, 1H), 5.80 (td, *J* = 17.0, 6.8 Hz, 1H), 5.36 (m, 1H), 5.01 (d, *J* = 12.1 Hz, 1H), 5.03–4.89 (m, 2H), 4.81 (d, *J* = 12.1 Hz, 1H), 4.20 (m, 1H), 3.79–3.38 (m, 3H), 2.27 (m, 2H), 2.07 (m, 4H), 1.87 (m, 2H), 1.74–1.66 (m, 1H), 1.62 (m, 2H), 1.48–1.37 (m, 2H), 1.29 (d, *J* = 6.9 Hz, 3H), 0.96 (d, *J* = 6.3 Hz, 3H), 0.93 (d, *J* = 6.9 Hz, 3H). LC/MS (*m*/*z*) 541.1 [M + H].

(*S*)-1-{(*S*)-2-[(*S*)-2-((2*R*,3*R*)-3-Methoxy-2-methyl-hept-6-enoylamino)-3-methyl-butyrylamino]-propionyl}-hexahydro-pyridazine-3-carboxylic acid (*R*)-1-(3-vinyl-phenyl)-ethyl ester (32)

A cooled (0 °C) solution of **30** (1.02 g, 1.735 mmol) in tetrahydrofuran/water (5:1, 36 mL) was treated with lithium hydroxide monohydrate (145.6 mg, 3.470 mmol). After stirring at 0 °C for 1.5 h, the reaction was quenched with hydrochloric acid (2 M, ~10 mL). The aqueous layer was extracted with ethyl acetate (2×). The combined organics were dried over anhydrous sodium sulfate, filtered, and the volatiles were removed *in vacuo*. Residual trichloroethanol was azeotroped off with toluene to provide crude (*S*)-1-{(*S*)-2-[(*S*)-2-((2*R*,3*R*)-3-methoxy-2-methyl-hept-6-enoylamino)-3-methyl-butyrylamino]-propionyl}-hexahydro-pyridazine-3-carboxylic acid (972 mg) as a white solid which was then combined with **21** (130.2 mg, 0.878 mmol), 4-dimethylaminopyridine (89.4 mg, 0.732 mmol) and dichloromethane (20 mL). The solution was then treated with 1-ethyl-3-(3-dimethylaminopropyl) carbodiimide (229.5 mg, 1.171 mmol). After stirring at room temperature for 3 h, silica gel was added and the volatiles were removed in vacuo. The residue was purified by silica gel chromatography using a 50 g Isolute cartridge

eluting with a continuous gradient of *iso*-hexane/ethyl acetate 1:0 to 0:1 to provide the title compound (195.1 mg, 45% over 2 steps) as a white solid. ^{1}H NMR (300 MHz, CD_3CN) δ 7.53–7.26 (m, 3H), 7.02 (d, J = 7.6 Hz, 1H), 6.79 (dd, J = 17.6, 10.9 Hz, 1H), 6.64 (d, J = 8.2 Hz, 1H), 5.95–5.79 (m, 3H), 5.29 (d, J = 11.1 Hz, 1H), 5.17 (*app* pentet, J = 7.1 Hz, 1H), 5.06 (dd, J = 17.2, 1.8 Hz, 1H), 4.96 (d, J = 10.5 Hz, 1H), 4.27 (d, J = 9.8 Hz, 1H), 4.19 (dd, J = 8.7, 5.8 Hz, 1H), 4.01–3.85 (m, 1H), 3.68–3.58 (m, 1H), 3.34 (dt, J = 7.1, 4.0 Hz, 1H), 3.31 (s, 3H), 3.21–3.02 (m, 1H), 2.56 (*app* pentet, J = 7.1 Hz, 1H), 2.14–2.06 (m, 3H), 1.80–1.59 (m, 5H), 1.58–1.47 (m, 4H), 1.21 (d, J = 6.9 Hz, 3H), 1.06 (d, J = 7.1 Hz, 3H), 0.91 (d, J = 6.9 Hz, 3H), 0.88 (d, J = 6.9 Hz, 3H). LC/MS (*m/z*) 585.3 [M+H], 607.3 [M+Na], Tr = 5.46 min.

(*R*)-1-(3-Vinylphenyl)ethyl (*S*)-1-(hept-6-enoyl-*L*-valyl-*L*-alanyl)hexahydropyridazine-3-carboxylate (33)

A cooled (0 °C) solution of **31** (330 mg, 0.61 mmol) in tetrahydrofuran/water mixture (5:1, 25 mL) was treated with lithium hydroxide monohydrate. After stirring at 0 °C for 1.5 h, the reaction was quenched with hydrochloric acid (1 M, ~5 mL). The aqueous layer was extracted with ethyl acetate (2×). The combined organics were dried over anhydrous sodium sulfate, filtered, and the volatiles were removed *in vacuo*. Residual trichloroethanol was azeotroped off with toluene to provide crude acid as a white solid which was then combined with **21** (99 mg, 0.67 mmol), 4-dimethylaminopyridine (112 mg, 0.91 mmol) and dichloromethane (10 mL). The solution was then treated with 1-ethyl-3-(3-dimethylaminopropyl) carbodiimide (140 mg, 0.73 mmol). After stirring at room temperature overnight, silica gel was added and the volatiles were removed *in vacuo*. The residue was purified by silica gel chromatography eluting with a continuous gradient of *iso*-hexane/ethyl acetate from 1:0 to 0:1 to provide the title compound

(302 mg, 92%) as a white solid. ^{1}H NMR (400 MHz, DMSO-d_6) δ 7.91–7.76 (m, 1H), 7.67–7.56 (m, 1H), 7.46–7.17 (m, 4H), 6.73 (dd, J = 17.7, 11.0 Hz, 1H), 5.92–5.67 (m, 3H), 5.35–5.26 (m, 2H), 5.20–4.81 (m, 4H), 4.22–4.08 (m, 1H), 3.68–3.54 (m, 1H), 2.23–2.07 (m, 3H), 2.06–1.83 (m, 3H), 1.77–1.53 (m, 2H), 1.52–1.41 (m, 4H), 1.39–1.25 (m, 3H), 1.15 (dd, J = 6.9, 1.4 Hz, 3H), 0.86–0.75 (m, 6H). LC/MS (*m*/*z*) 541.1 [M + H].

Construction of wild-type human cyclophilin A expression plasmids. Full length human petidylprolyl isomerase A (cyclophilin A) sequence (GenBank Accession # BC003026) was PCR-amplified from a template obtained from ATCC with the following 5′-TATACATatggtcaaccccaccgtgtt: and 3′ TTTTaagcttTTATTCGAGTTGTCCACAGT primers. The PCR product was digested with NdeI and HindIII restriction enzymes, gel purified using QIAquick Gel Extraction kit (Qiagen, Valencia, CA). The isolated fragment was subcloned into an in-house generated pET28a vector (EMD BioSciences, La Jolla, CA) with the insertion of an rTEV recognition site after an N-terminal 8 histidine tag. The construct pET28a-8H-Tev- Hu Cyp A (1-169) was sequence-verified prior to transformation into BL21 DE3 cells (Catalog #C6000-03, Invitrogen, Carlsbad, CA).

Expression of wild-type human cyclophilin A. A single colony of BL21DE3 harboring the plasmid pET28a-8H-Tev-Hu Cyp A (1-169) was inoculated into 200 ml of LB medium containing 50 μg/mL kanamycin and incubated overnight at 37 °C. The starter culture was then added to 18 liters of 2× YT medium containing 50 μg/mL kanamycin in a BioStatC Fermentor (Sartorius AG, Gottingen, Germany) at 37 °C until OD600 reached 1.0. Protein expression was induced by the addition of IPTG to a final concentration of 0.5 mM, when the temperature of the

culture dropped to 25 °C. Cell pellets expressing 8H-Tev-Hu CypA (hereafter designated simply as Cyp A) were harvested by centrifugation after 4 h.

Purification buffers. Buffer A contained 50 mM Tris-HCl pH 8.0, 1 M NaCl, 10 mM Imidazole HCl, 2 mM β-mercaptoethanol. Buffer B contained buffer A supplemented with 500 mM Imidazole HCl (Sigma). Buffer C contained 25 mM Tris pH 9.0, 10% Glycerol, 1mM DTT. Buffer D contained buffer C supplemented with 1M NaCl (Sigma).

Purification of wild-type human cyclophilin A. Cells containing Cyp A were resuspended in Buffer A supplemented with 1 mM PMSF at a ratio of 10 mL/g of cell pellet. The cells were lysed by 3 passages through an M-110L Microfluidizer Processor (Microfluidics, Newton, MA) set at 18,000 psi. Lysate was centrifuged at 12,000 × *g* for 1 h in a Beckman JLA8.100 rotor at 4 °C. The clarified supernatant was loaded to a 5 mL His-Trap HP (Catalog #17-5248-02, GE Healthcare, Piscataway, NJ) equilibrated in Buffer A. The His-trap HP column was washed with buffer A for 5 CV before elution with Buffer B using linear gradient from 10-500 mM Imidazole HCl. Eluted samples were analyzed by SDS-PAGE. Fractions containing Cyp A were pooled and dialyzed against 4 L of buffer C overnight at 4 °C. The dialyzed sample was loaded onto a 5 mL Q-HP HiTrap column (Catalog #17-1154-01, GE Healthcare, Piscataway, NJ) equilibrated in Buffer C. Following loading, the Q-HP column was washed to baseline before elution with a linear gradient from 0 to 800 mM NaCl with Buffer D. Samples were analyzed by SDS-PAGE before pooling the fractions containing Cyp A. The Cyp A pool was flash-frozen in liquid nitrogen, and stored at −80 °C.

Cyclophilin A TR-FRET competitive binding assay. Inhibitor potency was measured using a competitive binding assay with a time-resolved fluorescence resonance energy transfer (TR-FRET) readout. To a reaction buffer consisting of 35 mM HEPES pH 7.8, 100 mM NaCl, 0.01% NP-40 (Pierce), 1 mM DTT, and 1% DMSO were added the following: 5 nM of cyclophilin A modified at the N-terminus with an 8×histidine affinity tag (Cyp A); 150 nM of cyclosporin A modified at the sarcosine residue with a linker attached to a Cy5 fluorophore (CsA-Cy5); 1 nM Eu-labeled anti-(6×His) antibody (Perkin-Elmer); and test compound at one of various concentrations. The total volume of the assay solution was 100 μL. After a 2-h incubation, the TR-FRET was measured using a Perkin Elmer Envision plate reader (excitation at 340 nm, emission measured at 590 nm and 665 nm). The signal was calculated as the ratio of the emission at 665 nm to that at 590 nm. A K_d value was calculated using a 4-parameter logistic fit.

Peptidyl-prolyl isomerase functional assay. The assay was performed using an Agilent 8453 spectrophotometer essentially as described as the "uncoupled assay" by Janowski et al. [46] Assay buffer consisting of 35 mM HEPES pH 7.8 and 50 μM DTT was cooled to 10 °C (with stirring) in a precision glass cuvette and inhibitor was added from a 100% DMSO stock solution. A blank spectrum was obtained and then cyclophilin A as described above (f/c 2 nM) and tetra peptide substrate, Suc-Ala-Ala-Pro-Phe-*para*-nitroanilide dissolved in 0.5M LiCl in trifluoroethanol (Bachem, f/c 60 μM) were added and the change in absorbance measured over 5 min at 330 nM. A first order rate equation was fitted to the absorbance data to obtain a rate constant (first 10 to 15 s were eliminated due to mixing). The catalytic rate was calculated from the enzymatic rate minus the background rate. The K_i for an inhibitor was obtained from the rate constant plotted against the inhibitor concentration.

Cellular HCV replicon assays. Genotype 1b-Con1 HCV replicon cells were seeded into 384-well plates at a density of 2,000 cells/well as described previously.[47, 48] The assay plates were incubated for 72 h at 37 °C in an incubator under 5% CO_2 and 85% humidity, after which the cell culture medium was removed and the cells were assayed for luciferase activity as a marker for replicon levels. Luciferase activity was quantified by using a Renilla luciferase assay system (Promega). The 50% effective concentration (EC_{50}) for inhibiting replicon replication was determined by fitting the dose-response data with a 4-parameter logistic fit.

T cell proliferation assay. Human PBMCs were isolated from fresh whole blood derived from healthy donors (All Cells, Alameda, CA) using standard Ficoll density gradient separation techniques. Isolated PBMCs were labeled with 2.5 μM CellTrace violet cell proliferation dye (Thermo Fisher Scientific, Waltham, MA) for 20 min at 37 °C and excess of free dye was quenched with complete media containing RPMI 1640 (Corning, Corning, NY), 10% heat-inactivated fetal bovine serum (Hyclone Laboratories, Logan, UT) and 1% Penicillin-Streptomycin (Thermo Fisher Scientific). Washed, labeled PBMCs in complete media were plated at a density of 1×10^6 PBMCs per well into 96 well tissue culture plates pre-coated either with 5 μg/mL anti-human CD3 (clone OKT3; eBiosciences, San Diego, CA) in phosphate-buffered saline (PBS) or with PBS only. Compounds were added as an 11 point 4-fold serial dilution starting at a compound concentration of 10 μM. Plates were incubated for 4 days at 37 °C in an incubator under 5% CO_2 and 90% humidity, after which the PBMCs were harvested and stained with anti-human CD3 FITC antibody (clone UCHT1; BD Biosciences, San Jose, CA) for 30 min at RT in the dark. Washed, stained PBMCs were fixed with 4% paraformaldehyde and quantitated using a Fortessa X-20 flow cytometer (BD Biosciences). Data were analyzed with FlowJo software (FlowJo, Ashland, OR). The frequency of CD3+ T cells

with low CellTrace violet staining indicating T cell proliferation due to dye dilution was plotted using GraphPad Prism (GraphPad Software, San Diego, CA). The 50% effective concentration (EC_{50}) for inhibiting T cell proliferation was determined by fitting the concentration-response curve with a 3 parameter logistic fit.

Affinity measurments. Microcalorimetry experiments were performed using a MicroCal Auto-ITC200 calorimeter (MicroCal, Inc., Northampton, MA). Recombinant cyclophilin A was equilibrated by dialysis in a buffer containing 25 mM Hepes and 150 mM NaCl at pH 7.5 and diluted to a concentration of 15 μM protein. Compound stock solutions were prepared by dissolving the weighed powders in DMSO and then making the appropriate dilution (225 to 300 μM) in the experimental buffer, with the final concentration of DMSO being 3% (vol/vol). Experiments were performed at 25 °C. The measured binding K_a ,the change in enthalpy (ΔH), and the stoichiometry (N) were obtained by curve fitting using the software Origin (version 7.0; MicroCal Inc.). The change in Gibbs free energy (ΔG) and −TΔS (where T is temperature and ΔS is the change in entropy) were calculated using the measured K_a and ΔH values.[49]

Surface plasmon resonance. Variable-temperature surface plasmon resonance (SPR) experiments were performed using a Biacore T100 instrument and Series S NTA sensor chips. The NTA chips were loaded with nickel according to standard Biacore protocol. The His-Cyp A surfaces were constructed by first capturing His-Cyp A on the NTA chip and then performing a chemical coupling step as described by Wear et al.[50] Compounds **3**, **4**, and **5** were injected at a highest concentration of 1, 2, and 5 μM, respectively. For each compound, 3-fold serial dilutions were made to generate a total of 8 concentrations. Each concentration was injected for a 30-second association time and then monitored for a dissociation time of 120 seconds. Experiments

were run in HBS-EP pH7.4 (GE Healthcare) containing 1% DMSO and at a flow rate of 100 μL/min. Data were collected at 5, 10, 15, 20, 25, 30, 35, and 40 °C with 25 °C run in duplicate at both the beginning and end of the experiment. A 5-point DMSO concentration series (ranging from 0.5% to 1.5% DMSO), used to correct for excluded volume effects, was included after each temperature shift. Sensorgrams were double-referenced, corrected for solvent effects, and fit to a simple kinetic model using the Biacore T100 Evaluation software 2.0.2. Van't Hoff plots were then generated also using the same software to obtain values of ΔG°, ΔH°, and TΔS°. Errors cited represent standard errors of the mean derived from 3 independent Cyp A surfaces.

Conformational model. Compounds **3** and **5** were extracted from their respective cyclophilin bound crystal structures and subjected to the standard LigPrep procedure in Macromodel 10.3 (Schrodinger Release 2014.1). Conformations were generated with Macrocycle Conformational Sampling module[51] using the OPLS_2005 force field and GBSA for electrostatic treatment. Conformations were kept when energies were below 10 kcal/mol and no redundant conformation existed (RMSD >0.5 Å). 5000 simulation cycles were employed with 5000 LLMOD search steps. Since we were interested in having the conformational models for compounds **3** and **5** exhibit equal coverage, we used another pruning step using only the shared backbone atoms of the 2 macrocycles to compute RMSD values. Using the above criterion of >0.5 Å, this step eliminated a number of conformers for compound **3**. This procedure resulted in 120 conformers for compound **3** and 183 for compound **5**.

Crystallography methods. Compounds **3, 5, 6, 7,** and **8** were mixed with purified recombinant human Cyp A (20–30 mg/mL in 0.02 M HEPES pH 7.5, 0.1 M sodium chloride, and 0.01 M TCEP) at a 1.2:1 (compound:protein) molar ratio. All crystallization experiments followed

standard sitting drop vapor diffusion techniques. Crystals of Cyp A in complex with compound **3** were grown from a 1:1 mixture of protein-inhibitor solution to precipitant solution (0.1 M Tris-HCl pH 8.5, 0.1 M potassium chloride, and 2.2 M ammonium sulfate) and equilibrated against 100% precipitant solution. Crystals of Cyp A in complex with compound **5** were grown from a 1:1 mixture of protein-inhibitor solution to precipitant solution (0.05 M monobasic potassium phosphate and 20% (v/v) PEG 8000) and equilibrated against 100% precipitant solution. Crystals of Cyp A in complex with either compound **6** or **7** were grown from a 1:1 mixture of protein-inhibitor solution to precipitant solution (0.1 M sodium citrate pH 4.2 and 25% (v/v) PEG 3350) and equilibrated against 100% precipitant solution. Crystals of Cyp A in complex with compound **8** were grown from a 1:1 mixture of protein-inhibitor solution to precipitant solution (0.1 M Tris-HCl pH 8.5, 0.2 M potassium chloride and 2.0 M ammonium sulfate) and equilibrated against 100% precipitant solution. Crystals grown for approximately 1 week were harvested and flash frozen in cryogenic artificial mother liquor (respective precipitant solution supplemented with 15% (v/v) glycerol). X-ray diffraction data for each protein-inhibitor complex were collected on a single frozen (100 K) crystal on either beamline 5.0.1 or 5.0.2 at the Advanced Light Source (Berkeley, CA). All data were processed with HKL2000 and scaled with Scalepack.[52] A protein search model constructed using PDB entry 1CWA was used in the molecular replacement program, PHASER,[53] which found a unique solution for each protein-inhibitor complex. Initial models were refined using the PHENIX[54] suite of programs with manual model fitting. Ligands and ordered solvent molecules were included in the later stages of refinement. Unit cell descriptions as well as data collection and refinement statistics for all complexes are summarized in Tables S1 and S2.

ASSOCIATED CONTENT

Supporting Information. The following supporting information is available via the Internet at http://pubs.acs.org: Modeling data for **3** and **5**, and crystallographic data for **3**, **5**, **6**, **7**, and **8**; Molecular Formula Strings for **3-9.**

Accession Codes

Co-crystal structures of Cyp A with **3** (5T9U), **5** (5T9W), **6** (5T9Z), **7** (5TA2), and **8** (5TA4). Authors will release the atomic coordinates and experimental data upon article publication.

AUTHOR INFORMATION

Corresponding Author

*Brian.Schultz@gilead.com

(+1) 650 522-6349

Present Addresses

[¶]Currently at UCB, Avenue de l'Industrie, 1420 Braine-l'Alleud, Belgium

[#]Currently at Carbosynth, 8 & 9 Old Station Business Park, Compton, Berkshire, RG20 6NE, United Kingdom

Author Contributions

The manuscript was written through contributions of all authors. All authors have given approval to the final version of the manuscript.

Notes

The authors are current or former employees of Selcia, Ltd., Cypralis, Ltd., or Gilead Sciences, and may own company stock.

ACKNOWLEDGMENTS

We thank Becky Norquist for her assistance in preparing this manuscript. This work was funded by Selcia, Ltd. and Gilead Sciences.

ABBREVIATIONS

CsA, cyclosporine A; Cyp A, cyclophilin A; HCV, hepatitis C virus; HIV, human immunodeficiency virus; ITC, isothermal titration calorimetry; PPIase, peptidyl-prolyl isomerase; SPR, surface plasmon resonance

REFERENCES

1. Lang, K.; Schmid, F. X.; Fischer, G. Catalysis of protein folding by prolyl isomerase. *Nature* **1987,** *329*, 268-270.

2. Handschumacher, R. E.; Harding, M. W.; Rice, J.; Drugge, R. J.; Speicher, D. W. Cyclophilin: a specific cytosolic binding protein for cyclosporin A. *Science* **1984,** *226*, 544-547.

3. Fischer, G.; Wittmann-Liebold, B.; Lang, K.; Kiefhaber, T.; Schmid, F. X. Cyclophilin and peptidyl-prolyl cis-trans isomerase are probably identical proteins. *Nature* **1989,** *337*, 476-478.

4. Rosenwirth, B.; Billich, A.; Datema, R.; Donatsch, P.; Hammerschmid, F.; Harrison, R.; Hiestand, P.; Jaksche, H.; Mayer, P.; Peichl, P.; Quesniaux, V.; Schatz, F.; Schuurman, H.-J.; Traber, R.; Wenger, R.; Wolff, B.; Zenke, G.; Zurini, M. Inhibition of human immunodeficiency

virus type 1 replication by SDZ NIM 811, a nonimmunosuppressive cyclosporine analog. *Antimicrob. Agents Chemother.* **1994,** *38*, 1763-1772.

5. Traber, R.; Kobel, H.; Loosil, H.-R.; Senn, H.; Rosenwirth, B.; Lawen, A. [MeIle^4]Cyclosporin, a novel natural cyclosporin with anti-HIV activity: structural elucidation, biosynthesis and biological properties. *Antiviral Chem. Chemother.* **1994,** *5*, 331-339.

6. Nigro, P.; Pompilio, G.; Capogrossi, M. C. Cyclophilin A: a key player for human disease. *Cell Death Dis.* **2013,** *4*, e888.

7. Naoumov, N. V. Cyclophilin inhibition as potential therapy for liver diseases. *J. Hepatol.* **2014,** *61*, 1166-1174.

8. Elrod, J. W.; Molkentin, J. D. Physiologic functions of cyclophilin D and the mitochondrial permeability transition pore. *Circ. J.* **2013,** *77*, 1111-1122.

9. Fehr, T.; Kallen, J.; Oberer, L.; Sanglier, J. J.; Schilling, W. Sanglifehrins A, B, C and D, novel cyclophilin-binding compounds isolated from *Streptomyces* sp. A92-308110. II. Structure elucidation, stereochemistry and physico-chemical properties. *J. Antibiot. (Tokyo)* **1999,** *52*, 474-479.

10. Sanglier, J. J.; Quesniaux, V.; Fehr, T.; Hofmann, H.; Mahnke, M.; Memmert, K.; Schuler, W.; Zenke, G.; Gschwind, L.; Maurer, C.; Schilling, W. Sanglifehrins A, B, C and D, novel cyclophilin-binding compounds isolated from *Streptomyces* sp. A92-308110. I. Taxonomy, fermentation, isolation and biological activity. *J. Antibiot. (Tokyo)* **1999,** *52*, 466-473.

11. Zenke, G.; Strittmatter, U.; Fuchs, S.; Quesniaux, V. F.; Brinkmann, V.; Schuler, W.; Zurini, M.; Enz, A.; Billich, A.; Sanglier, J. J.; Fehr, T. Sanglifehrin A, a novel cyclophilin-

binding compound showing immunosuppressive activity with a new mechanism of action. *J. Immunol.* **2001,** *166*, 7165-7171.

12. Vuagniaux, G.; Hamel, A.; Crabbé, R.; Porchet, H. C.; Dumont, J.-M. Cyclophilin inhibitors. In *Antiviral Drug Strategies*, Wiley-VCH Verlag GmbH & Co. KGaA, Weinheim, Germany, 2011; pp 147-180.

13. Watashi, K.; Hijikata, M.; Hosaka, M.; Yamaji, M.; Shimotohno, K. Cyclosporin A suppresses replication of hepatitis C virus genome in cultured hepatocytes. *Hepatology* **2003,** *38*, 1282-1288.

14. Yang, F.; Robotham, J. M.; Nelson, H. B.; Irsigler, A.; Kenworthy, R.; Tang, H. Cyclophilin A is an essential cofactor for hepatitis C virus infection and the principal mediator of cyclosporine resistance in vitro. *J. Virol.* **2008,** *82*, 5269-5278.

15. Gaither, L. A.; Borawski, J.; Anderson, L. J.; Balabanis, K. A.; Devay, P.; Joberty, G.; Rau, C.; Schirle, M.; Bouwmeester, T.; Mickanin, C.; Zhao, S.; Vickers, C.; Lee, L.; Deng, G.; Baryza, J.; Fujimoto, R. A.; Lin, K.; Compton, T.; Wiedmann, B. Multiple cyclophilins involved in different cellular pathways mediate HCV replication. *Virology* **2010,** *397*, 43-55.

16. Puyang, X.; Poulin, D. L.; Mathy, J. E.; Anderson, L. J.; Ma, S.; Fang, Z.; Zhu, S.; Lin, K.; Fujimoto, R.; Compton, T.; Wiedmann, B. Mechanism of resistance of hepatitis C virus replicons to structurally distinct cyclophilin inhibitors. *Antimicrob. Agents Chemother.* **2010,** *54*, 1981-1987.

17. Yang, F.; Robotham, J. M.; Grise, H.; Frausto, S.; Madan, V.; Zayas, M.; Bartenschlager, R.; Robinson, M.; Greenstein, A. E.; Nag, A.; Logan, T. M.; Bienkiewicz, E.; Tang, H. A major

determinant of cyclophilin dependence and cyclosporine susceptibility of hepatitis C virus identified by a genetic approach. *PLoS Pathog.* **2010,** *6*, e1001118.

18. Hanoulle, X.; Badillo, A.; Wieruszeski, J. M.; Verdegem, D.; Landrieu, I.; Bartenschlager, R.; Penin, F.; Lippens, G. Hepatitis C virus NS5A protein is a substrate for the peptidyl-prolyl cis/trans isomerase activity of cyclophilins A and B. *J. Biol. Chem.* **2009,** *284*, 13589-13601.

19. Fernandes, F.; Ansari, I. U.; Striker, R. Cyclosporine inhibits a direct interaction between cyclophilins and hepatitis C NS5A. *PLoS One* **2010,** *5*, e9815.

20. Flisiak, R.; Horban, A.; Gallay, P.; Bobardt, M.; Selvarajah, S.; Wiercinska-Drapalo, A.; Siwak, E.; Cielniak, I.; Higersberger, J.; Kierkus, J.; Aeschlimann, C.; Grosgurin, P.; Nicolas-Metral, V.; Dumont, J. M.; Porchet, H.; Crabbe, R.; Scalfaro, P. The cyclophilin inhibitor Debio-025 shows potent anti-hepatitis C effect in patients coinfected with hepatitis C and human immunodeficiency virus. *Hepatology* **2008,** *47*, 817-826.

21. Flisiak, R.; Feinman, S. V.; Jablkowski, M.; Horban, A.; Kryczka, W.; Pawlowska, M.; Heathcote, J. E.; Mazzella, G.; Vandelli, C.; Nicolas-Metral, V.; Grosgurin, P.; Liz, J. S.; Scalfaro, P.; Porchet, H.; Crabbe, R. The cyclophilin inhibitor Debio 025 combined with PEG IFNalpha2a significantly reduces viral load in treatment-naive hepatitis C patients. *Hepatology* **2009,** *49*, 1460-1468.

22. Yu, M.; Peng, B.; Chan, K.; Gong, R.; Yang, H.; Delaney, W., 4th; Cheng, G. Robust and persistent replication of the genotype 6a hepatitis C virus replicon in cell culture. *Antimicrob. Agents Chemother.* **2014,** *58*, 2638-2646.

23. Novartis. *Novartis Q1 2012 Interim Financial Report – Supplementary Data*; 2012.

24. Scribner, A.; Houck, D.; Huang, Z.; Mosier, S.; Peel, M.; Scorneaux, B. Synthesis and biological evaluation of [D-lysine]^{8}cyclosporin A analogs as potential anti-HCV agents. *Bioorg. Med. Chem. Lett.* **2010**, *20*, 6542-6546.

25. Hopkins, S.; Scorneaux, B.; Huang, Z.; Murray, M. G.; Wring, S.; Smitley, C.; Harris, R.; Erdmann, F.; Fischer, G.; Ribeill, Y. SCY-635, a novel nonimmunosuppressive analog of cyclosporine that exhibits potent inhibition of hepatitis C virus RNA replication *in vitro*. *Antimicrob. Agents Chemother.* **2010**, *54*, 660-672.

26. Hopkins, S.; DiMassimo, B.; Rusnak, P.; Heuman, D.; Lalezari, J.; Sluder, A.; Scorneaux, B.; Mosier, S.; Kowalczyk, P.; Ribeill, Y.; Baugh, J.; Gallay, P. The cyclophilin inhibitor SCY-635 suppresses viral replication and induces endogenous interferons in patients with chronic HCV genotype 1 infection. *J. Hepatol.* **2012**, *57*, 47-54.

27. Sedrani, R.; Kallen, J.; Martin Cabrejas, L. M.; Papageorgiou, C. D.; Senia, F.; Rohrbach, S.; Wagner, D.; Thai, B.; Jutzi Eme, A. M.; France, J.; Oberer, L.; Rihs, G.; Zenke, G.; Wagner, J. Sanglifehrin-cyclophilin interaction: degradation work, synthetic macrocyclic analogues, X-ray crystal structure, and binding data. *J. Am. Chem. Soc.* **2003,** *125*, 3849-3859.

28. Wiedmann, B.; Puyang, X.; Poulin, D.; Mathy, J. E.; Ma, S.; Anderson, L. J.; Fujimoto, R.; Compton, T. G.; Lin, K. Characterization of mechanism of resistance to cyclophilin inhibitors in HCV replicon. Presented at the 15th International Symposium on Hepatitis C Virus and Related Viruses, San Antonio, TX, October 5-9, 2008; Poster #305.

29. Gregory, M. A.; Bobardt, M.; Obeid, S.; Chatterji, U.; Coates, N. J.; Foster, T.; Gallay, P.; Leyssen, P.; Moss, S. J.; Neyts, J.; Nur-e-Alam, M.; Paeshuyse, J.; Piraee, M.; Suthar, D.; Warneck, T.; Zhang, M. Q.; Wilkinson, B. Preclinical characterization of naturally occurring polyketide cyclophilin inhibitors from the sanglifehrin family. *Antimicrob. Agents Chemother.* **2011,** *55*, 1975-1981.

30. Moss, S. J.; Bobardt, M.; Leyssen, P.; Coates, N.; Chatterji, U.; Dejian, X.; Foster, T.; Liu, J.; Nur-e-Alam, M.; Suthar, D.; Yongsheng, C.; Warneck, T.; Zhang, M.-Q.; Neyts, J.; Gallay, P.; Wilkinson, B.; Gregory, M. A. Sangamides, a new class of cyclophilin-inhibiting host-targeted antivirals for treatment of HCV infection. *Med. Chem. Comm.* **2012,** *3*, 944-949.

31. Hansson, M. J.; Moss, S. J.; Bobardt, M.; Chatterji, U.; Coates, N.; Garcia-Rivera, J. A.; Elmer, E.; Kendrew, S.; Leyssen, P.; Neyts, J.; Nur, E. A. M.; Warneck, T.; Wilkinson, B.; Gallay, P.; Gregory, M. A. Bioengineering and semisynthesis of an optimized cyclophilin inhibitor for treatment of chronic viral infection. *Chem. Biol.* **2015,** *22*, 285-292.

32. Sweeney, Z. K.; Fu, J.; Wiedmann, B. From chemical tools to clinical medicines: nonimmunosuppressive cyclophilin inhibitors derived from the cyclosporin and sanglifehrin scaffolds. *J. Med. Chem.* **2014,** *57*, 7145-7159.

33. McQuaid, T.; Savini, C.; Seyedkazemi, S. Sofosbuvir, a significant paradigm change in HCV treatment. *J. Clin. Transl. Hepatol.* **2015,** *3*, 27-35.

34. Nicolaou, K. C.; Xu, J.; Murphy, F.; Barluenga, S.; Baudoin, O.; Wei, H.; Gray, D. L.; Ohshima, T. Total synthesis of sanglifehrin A. *Angew. Chem. Int. Ed. Engl.* **1999,** *38*, 2447-2451.

35. Duan, M.; Paquette, L. A. Enantioselective total synthesis of the cyclophilin-binding immunosuppressive agent sanglifehrin A. *Angew. Chem. Int. Ed. Engl.* **2001,** *40*, 3632-3636.

36. Paquette, L. A.; Duan, M.; Konetzki, I.; Kempmann, C. A convergent three-component total synthesis of the powerful immunosuppressant (-)-sanglifehrin A. *J. Am. Chem. Soc.* **2002,** *124*, 4257-4270.

37. Martin Cabrejas, L. M.; Rohrbach, S.; Wagner, D.; Kallen, J.; Zenke, G.; Wagner, J. Macrolide analogues of the novel immunosuppressant sanglifehrin: new application of the ring-closing metathesis reaction. *Angew. Chem. Int. Ed. Engl.* **1999,** *38*, 2443-2446.

38. Wagner, J.; Martin Cabrejas, L. M.; Grossmith, C. E.; Papageorgiou, C.; Senia, F.; Wagner, D.; France, J.; Nolan, S. P. Synthesis of macrolide analogues of sanglifehrin by RCM: unique reactivity of a ruthenium carbene complex bearing an imidazol-2-ylidene ligand. Ring-closing metathesis. *J. Org. Chem.* **2000,** *65*, 9255-9260.

39. Paterson, I.; Norcross, R. D.; Ward, R. A.; Romea, P.; Lister, M. A. Studies in macrolide synthesis: a stereocontrolled synthesis of oleandolide employing reagent- and substrate-controlled aldol reactions of (*S*)-1-(benzyloxy)-2-methylpentan-3-one. *J. Am. Chem. Soc.* **1994,** *116*, 11287-11314.

40. Banteli, R.; Wagner, J.; Zenke, G. Synthesis of derivatives of the novel cyclophilin-binding immunosuppressant sanglifehrin A with reduced numbers of polar functions. *Bioorg. Med. Chem. Lett.* **2001,** *11*, 1609-1612.

41. Steadman, V. A.; Poullennec, K. G.; Lazarides, L.; Aciro, C.; Dean, D. K.; Keats, A. J.; Siegel, D. S.; Schrier, A. J.; Mackman, R.; Jansa, P.; Watt, G.; Highton, A. J.; Chiva, J. Y.

Macrocyclic Inhibitors of Flaviviridae Viruses. International Patent WO 2013185093 A1 20131212, 2013.

42. Aciro, C.; Steadman, V. A.; Pettit, S. N.; Poullennec, K. G.; Lazarides, L.; Dean, D. K.; Dunbar, N. A.; Highton, A. J.; Keats, A. J.; Siegel, D. S.; Karki, K. K.; Schrier, A. J.; Jansa, P.; Mackman, R.; Chiva, J. Y. Macrocyclic Inhibitors of Flaviviridae Viruses. International Patent WO 2013185103 A1 20131212, 2013.

43. Aciro, C.; Steadman, V. A.; Pettit, S. N.; Poullennec, K. G.; Lazarides, L.; Dean, D. K.; Dunbar, N. A.; Highton, A. J.; Keats, A. J.; Siegel, D. S.; Karki, K. K.; Schrier, A. J.; Jansa, P.; Mackman, R. Macrocyclic Inhibitors of Flaviviridae Viruses. International Patent WO 2013185090 A1 20131212, 2013.

44. Appleby, T.; Fliri, H. G.; Keats, A. J.; Lazarides, L.; Mackman, R. L.; Pettit, S. N.; Poullennec, K. G.; Sanvoisin, J.; Steadman, V. A.; Watt, G. M. Macrocyclic Inhibitors of Flaviviridae Viruses. International Patent WO 2012078915 A1 20120614, 2012.

45. Zhou, G.; Hu, Q. Y.; Corey, E. J. Useful enantioselective bicyclization reactions using an N-protonated chiral oxazaborolidine as catalyst. *Org. Lett.* **2003,** *5*, 3979-3982.

46. Janowski, B.; Wollner, S.; Schutkowski, M.; Fischer, G. A protease-free assay for peptidyl prolyl cis/trans isomerases using standard peptide substrates. *Anal. Biochem.* **1997,** *252*, 299-307.

47. Robinson, M.; Yang, H.; Sun, S. C.; Peng, B.; Tian, Y.; Pagratis, N.; Greenstein, A. E.; Delaney, W. E., 4th. Novel hepatitis C virus reporter replicon cell lines enable efficient antiviral screening against genotype 1a. *Antimicrob. Agents Chemother.* **2010,** *54*, 3099-3106.

48. Fenaux, M.; Eng, S.; Leavitt, S. A.; Lee, Y. J.; Mabery, E. M.; Tian, Y.; Byun, D.; Canales, E.; Clarke, M. O.; Doerffler, E.; Lazerwith, S. E.; Lew, W.; Liu, Q.; Mertzman, M.; Morganelli, P.; Xu, L.; Ye, H.; Zhang, J.; Matles, M.; Murray, B. P.; Mwangi, J.; Zhang, J.; Hashash, A.; Krawczyk, S. H.; Bidgood, A. M.; Appleby, T. C.; Watkins, W. J. Preclinical characterization of GS-9669, a thumb site II inhibitor of the hepatitis C virus NS5B polymerase. *Antimicrob. Agents Chemother.* **2013,** *57*, 804-810.

49. Sigurskjold, B. W. Exact analysis of competition ligand binding by displacement isothermal titration calorimetry. *Anal. Biochem.* **2000,** *277*, 260-266.

50. Wear, M. A.; Patterson, A.; Malone, K.; Dunsmore, C.; Turner, N. J.; Walkinshaw, M. D. A surface plasmon resonance-based assay for small molecule inhibitors of human cyclophilin A. *Anal. Biochem.* **2005,** *345*, 214-226.

51. Watts, K. S.; Dalal, P.; Tebben, A. J.; Cheney, D. L.; Shelley, J. C. Macrocycle conformational sampling with MacroModel. *J. Chem. Inf. Model.* **2014,** *54*, 2680-2696.

52. Otwinowski, Z.; W., M. Processing of X-ray diffraction data collected in oscillation mode. *Methods Enzymol.* **1997,** *276*, 307-326.

53. McCoy, A. J.; Grosse-Kunstleve, R. W.; Adams, P. D.; Winn, M. D.; Storoni, L. C.; Read, R. J. Phaser crystallographic software. *J. Appl. Crystallogr.* **2007,** *40*, 658-674.

54. Adams, P. D.; Afonine, P. V.; Bunkoczi, G.; Chen, V. B.; Davis, I. W.; Echols, N.; Headd, J. J.; Hung, L. W.; Kapral, G. J.; Grosse-Kunstleve, R. W.; McCoy, A. J.; Moriarty, N. W.; Oeffner, R.; Read, R. J.; Richardson, D. C.; Richardson, J. S.; Terwilliger, T. C.; Zwart, P.

H. PHENIX: a comprehensive Python-based system for macromolecular structure solution. *Acta Crystallogr., Sect. D: Biol. Crystallogr.* **2010,** *66*, 213-221.

Table 1. Biochemical and Cellular Potency of Cyclophilin Inhibitors **3-9**

Compound	TR-FRET cyclophilin A binding K_d, nM	PPIase functional assay K_i, nM	HCV genotype 1b replicon EC_{50}, nM
3	25	16	600
4	65	65	240
5	2600	795	4500
6	64	14	320
7	11	4	36
8	24	7	87
9	48	4.3	620
CsA	17	6.7	170

CsA, cyclosporine A; PPIase, peptidyl-prolyl isomerase; TR-FRET, time-resolved fluorescence resonance energy transfer

Table 2. Thermodynamic Parameters for Binding of Compounds **3-5** to Cyclophilin A.

	Compound **3**		Compound **4**		Compound **5**	
	ITC	SPR	ITC	SPR	ITC	SPR
ΔG (cal/mol)	-10300 ± 100	-10610 ± 30	-9500 ± 100	-10000 ± 100	-8200 ± 200	-8500 ± 100
ΔH (cal/mol)	-9970 ± 60	-12600 ± 1200	-8600 ± 100	-8100 ± 500	-7000 ± 400	-5400 ± 700
-TΔS (cal/mol)	-320 ± 30	2100 ± 1200	-930 ± 140	-1800 ± 500	-1200 ± 600	-2700 ± 600
N (ITC)	0.97 ± 0.01		0.996 ± 0.003		1.00 ± 0.03	

ITC, isothermal titration calorimetry; SPR, surface plasmon resonance

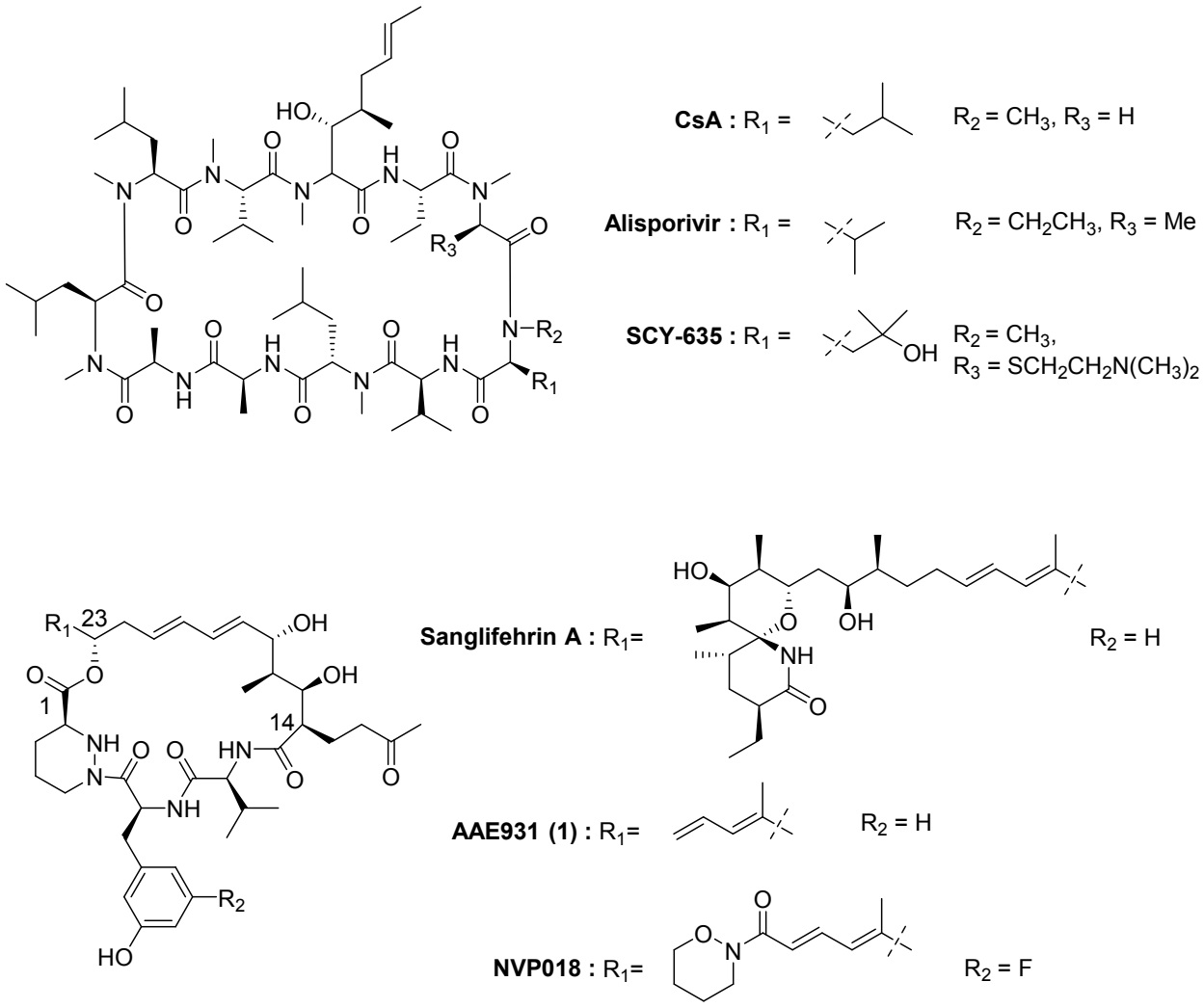

Figure 1. Structures of cyclosporin and sanglifehrin analogs.

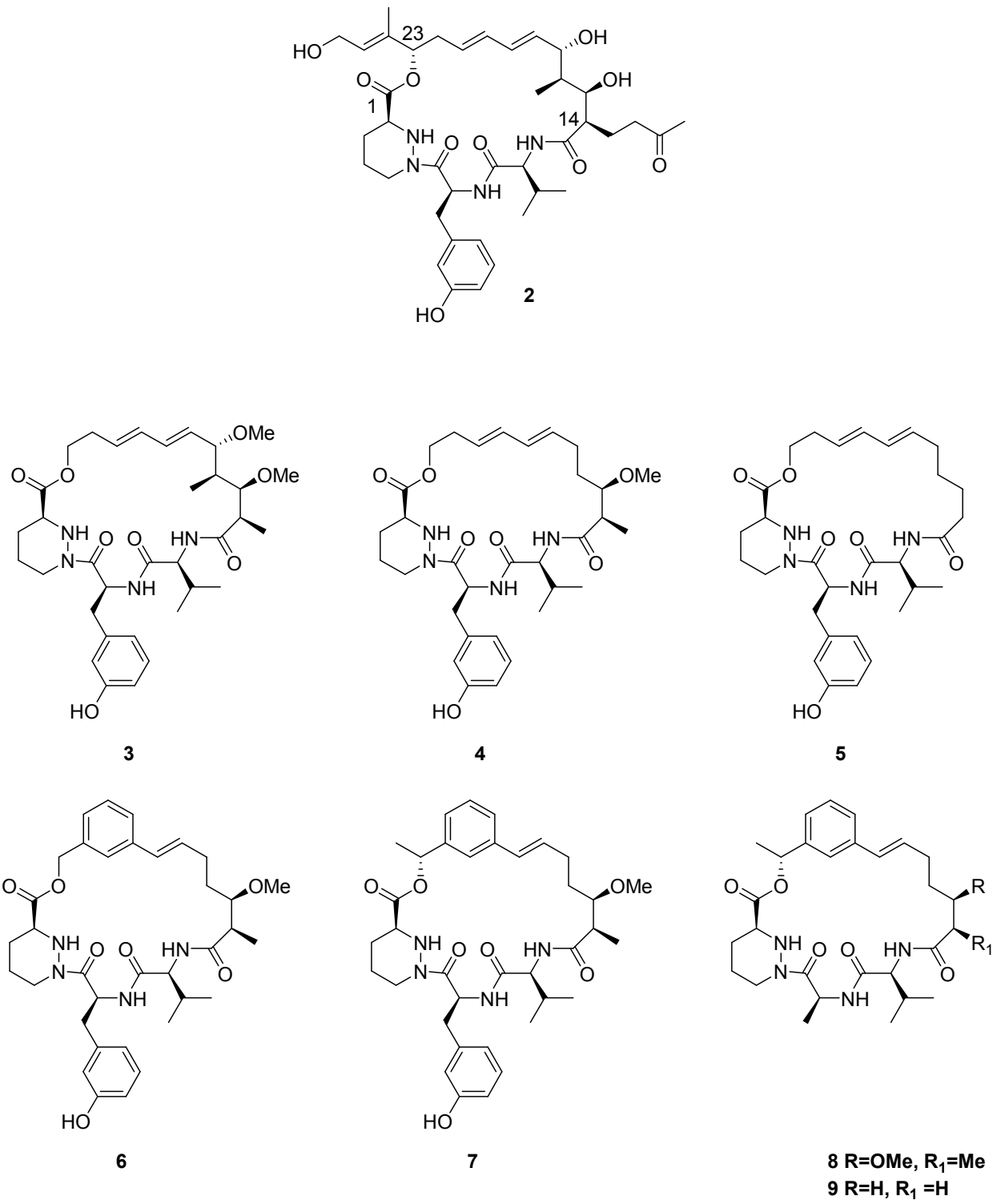

Figure 2. Simplified sanglifehrin macrocycles based on **2.**

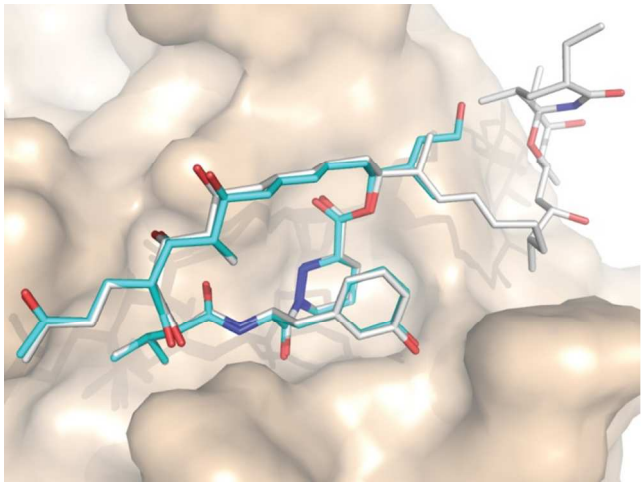

Figure 3. Overlay of **2** (cyan) and sanglifehrin A (light gray) bound to human cyclophilin A. The coordinates used to generate the superposition were retrieved from the Protein Data Bank (http://www.rcsb.org/pdb/home/home.do) under the accession codes 1NMK (**2** complex) and 1YND (sanglifehrin A complex).

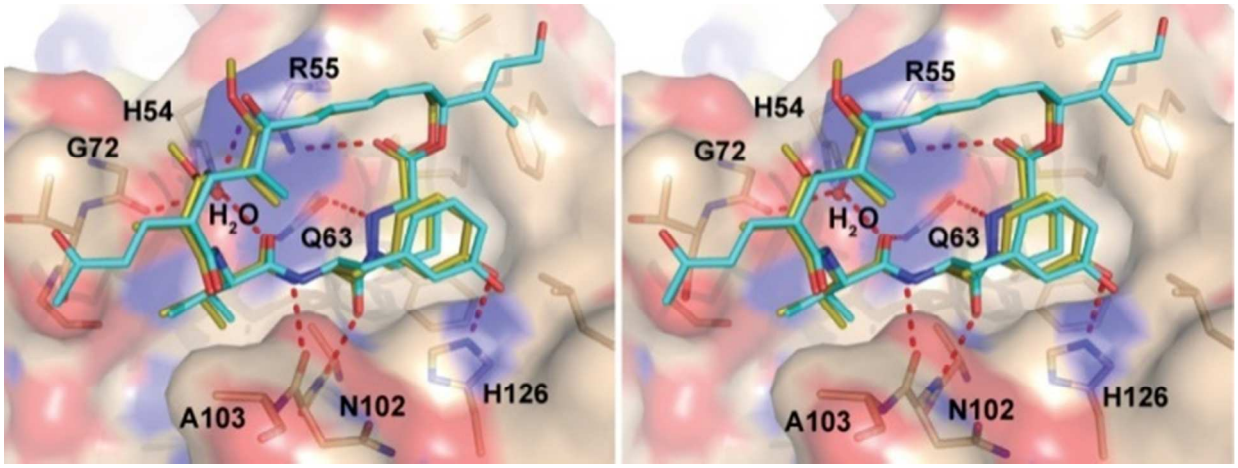

Figure 4. A stereoscopic view of compound **3** (gold) bound to cyclophilin A superimposed on the **2** (cyan) protein-inhibitor complex (PDB accession code 1NMK). Active-site residues participating in polar interactions with the ligand or structural water (red, H_2O) are shown as sticks and colored according to atom type (red, oxygen; blue, nitrogen; beige, carbon). Hydrogen bonds based on heavy atom distances (<3.2 Å) are indicated by dashed red lines.

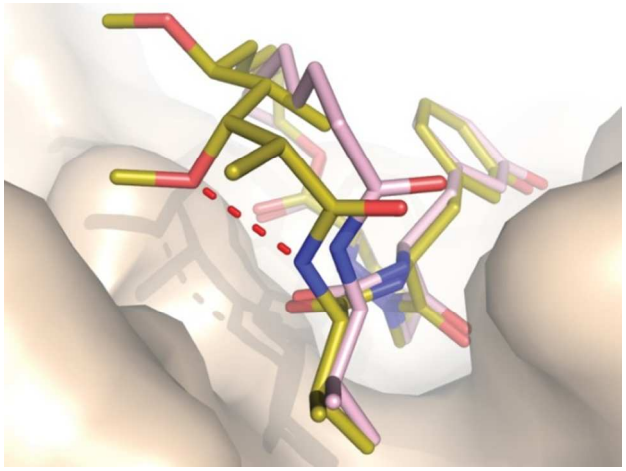

Figure 5. An overlay of the compound **3** (gold) and compound **5** (pink) protein-inhibitor complex structures highlighting the differences in conformation for the non-peptidic region of the compounds and the intramolecular H-bond (dashed red line) observed in compound **3**.

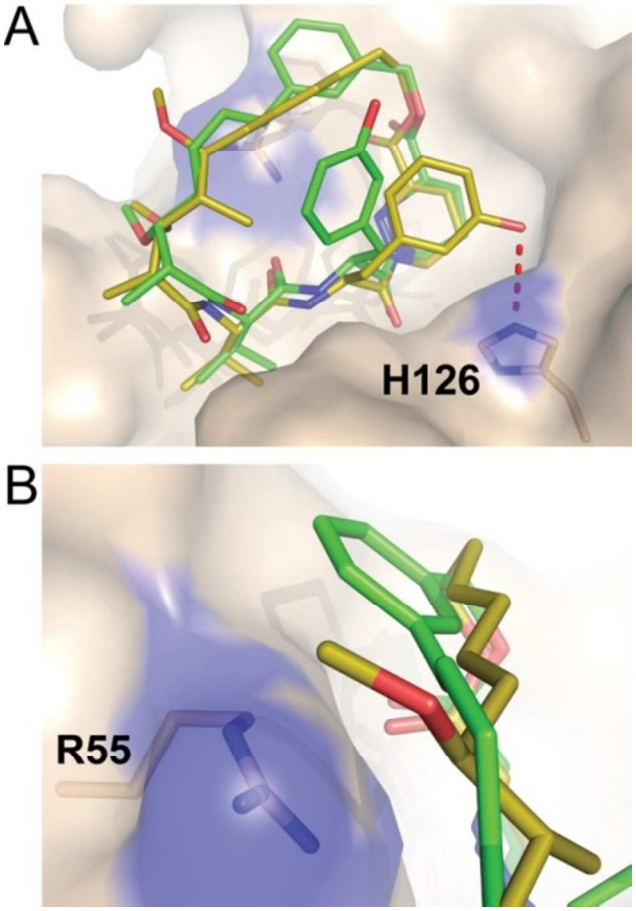

Figure 6. Overlay of the compound **3** (gold) and compound **6** (green) protein-inhibitor complex structures highlighting (A) the rotation of the *m*-Tyr sidechain resulting in the subsequent loss of the H-bond to His126 and (B) the stacking of the styrene group with the guanidinium group of Arg55.

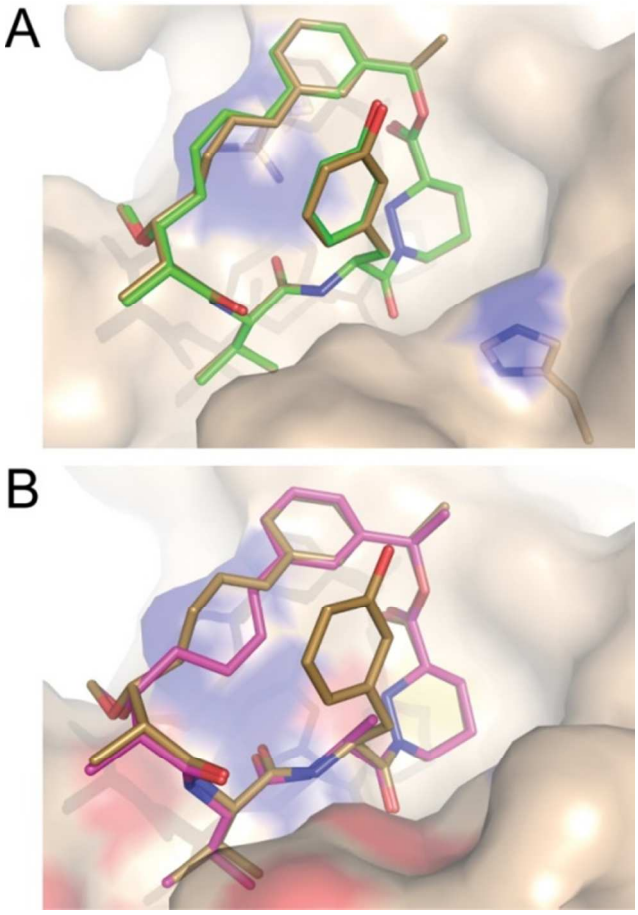

Figure 7. Comparisons of the cyclophilin-bound conformations for (A) Compounds **6** (green) and **7** (light brown) and for (B) compounds **7** (light brown) and **8** (magenta).

Scheme 1. Synthesis of **3**.

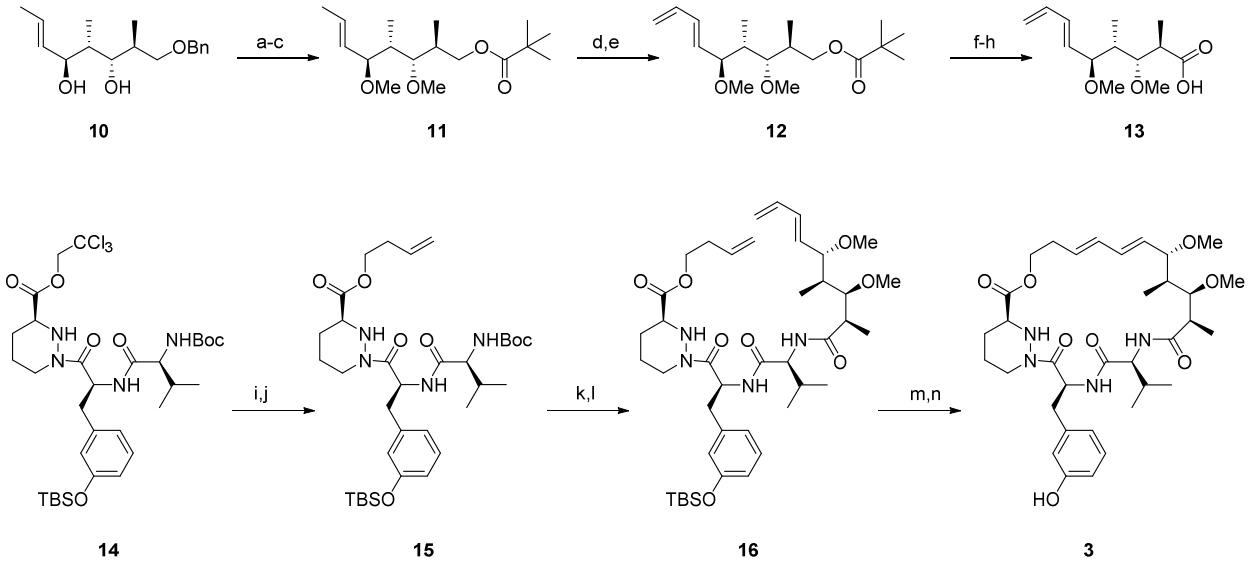

[a] Reagents and conditions: (a) 18-C-6, THF, KH (30% b/w), MeI, 91%; (b) LiDBB, THF, 93%; (c) PivCl, Py, 100%; (d) O_3, DCM, PPh_3, 81%; (e) diethyl allylphosphonate, THF, *n*-BuLi, DMPU, 60%; (f) NaOMe, MeOH, 100%; (g) TPAP, NMO, 4Å sieves, DCM, 93%; (h) $NaClO_2$, NaH_2PO_4, 2-Me-2-butene, H_2O, *t*-BuOH, 79%; (i) Zn, NH_4OAc, THF, H_2O; (j) Et_3N, 2,4,6-trichlorobenzoylchloride, homoallyl alcohol, 4-DMAP, PhMe 14% 2 steps; (k) TMSOTf, DCM, *i*-Pr_2NEt; (l) **13**, HATU, *i*-Pr_2NEt, DMF, 70% 2 steps; (m) Grubbs I, DCM; (n) TBAF, THF, 14% 2 steps.

Scheme 2. Synthesis of **4**, **6**, and **7**.

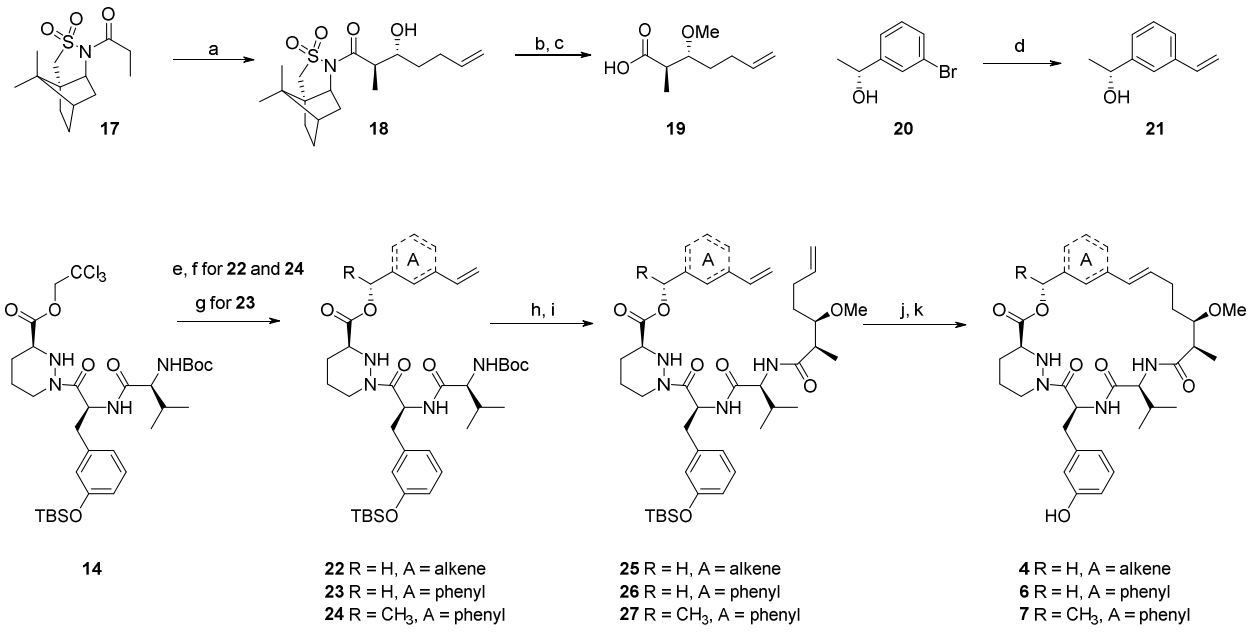

[a] Reagents and conditions: (a) t-$BuMe_2SiOTf$, Et_3N, CaH_2, DCM; 4-pentenal, $TiCl_4$, DCM, 60%; (b) Proton sponge, Me_3OBF_4, DCM, 86%; (c) LiOH, THF, H_2O, 66%; (d) (a) Tri-n-butyl(vinyl)tin, $PdCl_2(Ph_3P)_2$, PhMe, 89%; (e) Zn, NH_4OAc, THF, H_2O; (f) 2,4,6-trichlorobenzoyl chloride Et_3N, (*E*)-hexa-3,5-dien-1-ol, 4-DMAP, PhMe, 70% over 2 steps for **22**; EDC, 4-DMAP, DCM, **21**, 54% over 2 steps for **24**; (g) NaH (60% wt), (3-vinyl-phenyl)-methanol, THF, 59% for **23**; (h) TMSOTf, DCM, *i*-Pr_2NEt; (i) HATU, *i*-Pr_2NEt, DMF, **19**, 37% over 2 steps for **25,** and 78% over 2 steps for **26**; EDC, HOBt, CH_3CN, **19**, 55% over 2 steps for **27**; (j) Grubbs I, DCM for **24** and **75%** for **25**; Hoveyda-Grubbs II, DCM, 63% for **26**; (k) TBAF, THF, 44-63%.

Scheme 3. Synthesis of **8** and **9**.

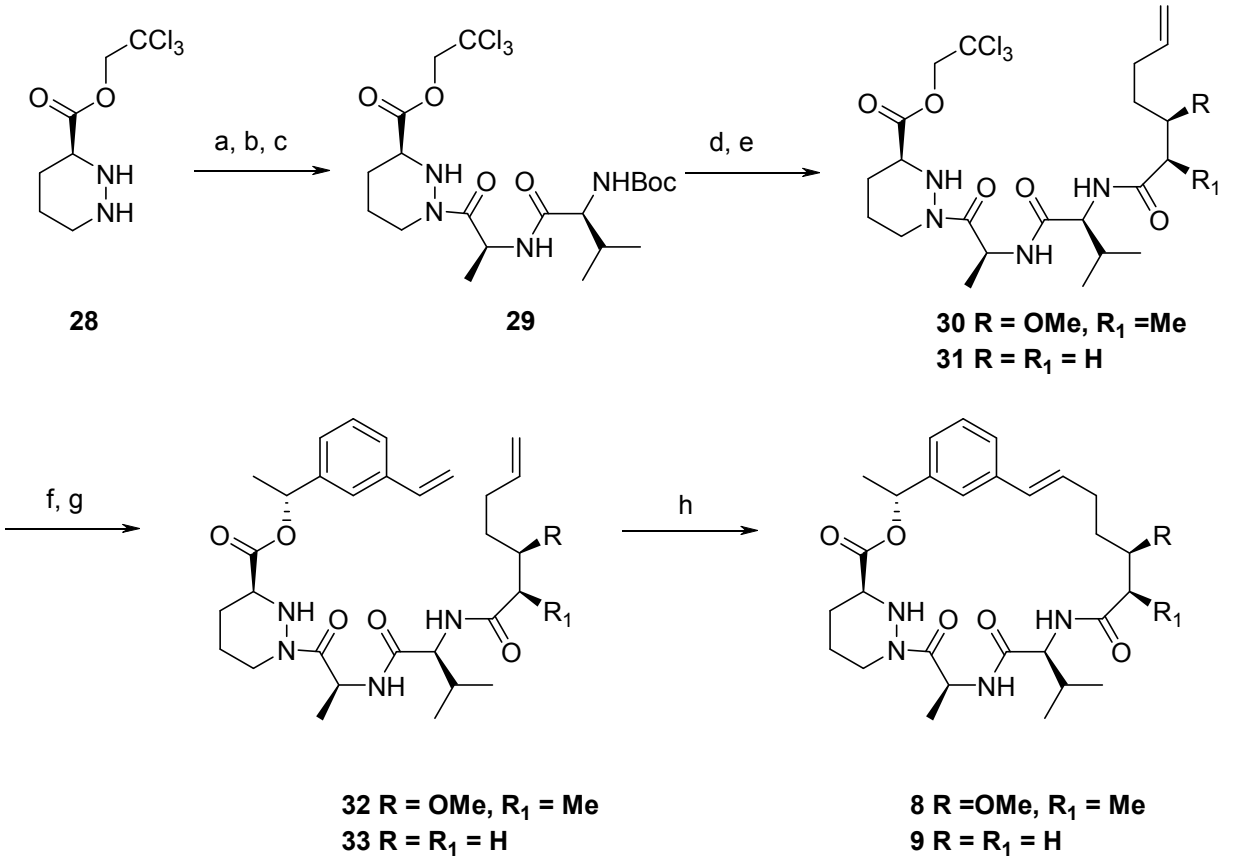

[a] Reagents and conditions: (a) HBTU, *i*-Pr_2NEt, Boc-Ala, CH_3CN, 92%; (b) TFA, DCM; (c) HBTU, *i*-Pr_2NEt, CH_3CN, Boc-Val, 92% 2 steps; (d) TMSOTf, DCM, *i*-Pr_2NEt; (e) EDC, HOBt, CH_3CN, **19**, 77% over 2 steps for **30**; HATU, *i*-Pr_2NEt, CH_3CN, hept-6-enoic acid, 75% over 2 steps for **31**; (f) LiOH, THF, H_2O; (g) EDC, 4-DMAP, **21**, DCM, 45% over 2 steps for **32;** 92% over 2 steps for **33**; (h) Hoveyda-Grubbs II, DCE, 28 % for **8**; 22% for **9**.

Table of Contents graphic